



Triarylmethanes, a new class of Cx50 inhibitors

Silke B. Bodendiek¹, Clio Rubinos², Maria Pilar Trelles², Nichole Coleman¹, David Paul Jenkins¹, Heike Wulff^{1†} and Miduturu Srinivas^{2*†}

¹ Department of Pharmacology, University of California, Davis, CA, USA

² Department of Biological Sciences, State University of New York College of Optometry, New York, NY, USA

Edited by:

Michael Pusch, Istituto di Biofisica, Consiglio Nazionale delle Ricerche, Italy

Reviewed by:

Alonso P. Moreno, Cardiovascular and Training Institute at the University of Utah, USA

Andrew L. Harris, New Jersey Medical School, USA

James Hall, University of California, Irvine, USA

*Correspondence:

Miduturu Srinivas, Department of Biological Sciences, State University of New York – State College of Optometry, 33W 42nd Street, New York, NY 10036, USA.

e-mail: msrinivas@sunyopt.edu

[†] Heike Wulff and Miduturu Srinivas have contributed equally to this work.

The paucity of specific pharmacological agents has been a major impediment for delineating the roles of gap junction (GJ) channels formed by connexin proteins in physiology and pathophysiology. Here, we used the selective optimization of side activities (SOSA) approach, which has led to the design of high affinity inhibitors of other ion channels, to identify a specific inhibitor for channels formed by Cx50, a connexin subtype that is primarily expressed in the lens. We initially screened a library of common ion channel modulating pharmacophores for their inhibitory effects on Cx50 GJ channels, and identified four new classes of compounds. The triarylmethane (TRAM) clotrimazole was the most potent Cx50 inhibitor and we therefore used it as a template to explore the structure activity relationship (SAR) of the TRAMs for Cx50 inhibition. We describe the design of T122 (*N*-[(2-methoxyphenyl)diphenylmethyl]-1,3-thiazol-2-amine) and T136 (*N*-[(2-iodophenyl)diphenylmethyl]-1,3-thiazol-2-amine), which inhibit Cx50 with IC₅₀s of 1.2 and 2.4 μM. Both compounds exhibit at least 10-fold selectivity over other connexins as well as major neuronal and cardiac voltage-gated K⁺ and Na⁺ channels. The SAR studies also indicated that the TRAM pharmacophore required for connexin inhibition is significantly different from the pharmacophore required for blocking the calcium-activated KCa3.1 channel. Both T122 and T136 selectively inhibited Cx50 GJ channels in lens epithelial cells, suggesting that they could be used to further explore the role of Cx50 in the lens. In addition, our results indicate that a similar approach may be used to find specific inhibitors of other connexin subtypes.

Keywords: connexin 50, gap junctions, triarylmethane, inhibitors, pharmacophore, channel, SAR, lens

INTRODUCTION

Connexins (Cx) are a family of proteins with four transmembrane regions, which are encoded by 21 genes in humans and which form hexameric connexons (= hemichannels). These connexons can either function as transmembrane ion channels or assemble into gap junctions (GJ) by the docking of two hemichannels from adjacent cells and directly mediate signaling between cells by passing ions, metabolites and signaling molecules up to 1 kDa in mass. Both hemichannels and GJ channels formed by different connexins play important roles in tissue homeostasis and have therefore been proposed as potential new targets for the treatment of epilepsy, cardiac arrhythmia, cancer, stroke, essential tremor, and corneal wound healing (Nemani and Binder, 2005; Salameh and Dhein, 2005; Bodendiek and Raman, 2010; Kandouz and Batist, 2010).

Since the 1980s several endogenous as well as exogenous molecules that modulate GJ channels have been discovered. The peptidic GJ channel activator rotigaptide, which mainly activates Cx43, advanced into clinical trials for the treatment of atrial fibrillation (phase II, terminated in 2007) and endothelial dysfunction (Lang et al., 2008), while GAP-134, an orally available di-peptidic analog of rotigaptide, recently completed phase I clinical trials for the treatment of atrial fibrillation (ClinicalTrials.gov). However, apart from these exceptions, the development of GJ channel modulators as pharmacological tools and potential therapeutics is still

in its infancy. Most existing modulators are either of low potency and exhibit little selectivity either for connexin channels or among individual connexin subtypes. For example, one of the most commonly used GJ channel blockers, carbenoxolone, a more water soluble derivative of the pentacyclic triterpenoid glycyrrhetic acid, reversibly inhibits GJ currents in human fibroblasts with an IC₅₀ of 3 μM and reduces Cx26 and Cx38 hemichannel currents in *Xenopus* oocytes with IC₅₀s of 21 and 34 μM, respectively. However, at similar concentrations carbenoxolone also inhibits several other targets such as the enzyme 11β-hydroxysteroid dehydrogenase (IC₅₀ ~5 μM; Monder et al., 1989), voltage-gated Ca²⁺ currents (IC₅₀ 48 μM; Vessey et al., 2004), and the structurally similar pannexin channels (IC₅₀ 2–5 μM; Locovei et al., 2007). At even lower concentrations carbenoxolone inhibits P2x7 receptors (IC₅₀ 175 nM; Suadicani et al., 2006). Other commonly used connexin blockers like the long-chain alcohols heptanol and octanol, the diphenylborate 2-APB or flufenamic acid are similarly either of low potency or lack selectivity for connexin channels (for a recent review see: Bodendiek and Raman, 2010).

Potent connexin subtype selective modulators are urgently needed to further elucidate the physiological and pathophysiological roles of the different connexins and to perform proof-of-concept studies validating connexins as potential drug targets for various diseases for which they have been proposed as novel

targets. We therefore screened a small library of compounds containing ion channel modulating pharmacophores for their effects on Cx50 GJ channels. Cx50 was used as an exemplary connexin because it is expressed robustly in expression systems. Cx50 is mainly expressed in the crystalline lens. In lens epithelial cells, it is co-expressed with Cx43 and plays an important role in post-natal lens growth (White et al., 1998; Rong et al., 2002). In fiber cells, where it is co-expressed with Cx46, it has been shown to be an important component of the lens microcirculation, essential for maintenance of lens transparency (Mathias et al., 1997, 2010). Genetic deletion of Cx50 causes mild cataracts and significantly decreases lens growth (White et al., 1998; Rong et al., 2002), while missense and frame shift mutations have been found in families with inherited cataracts (Berthoud and Beyer, 2009; Mathias et al., 2010). To further study the role of Cx50 channels in the lens, a potent and selective blocker would be of great interest. Such an inhibitor is likely to be useful to dissect the contribution of the coupling provided by Cx50 to lens development and transparency. In this study, we describe the design of two Cx50 inhibitors with IC₅₀s of 1.2 and 2.4 μM. Both compounds exhibit excellent selectivity for Cx50 over Cx43, and Cx46, which are also expressed in the lens (<18% inhibition at 10 μM), and strongly reduced junctional currents in primary lens epithelial cells isolated on postnatal day 6, a developmental time-point where Cx50 provides the majority of the coupling in the epithelium. These new pharmacological tool compounds will be useful to further explore the role of Cx50 in lens physiology and pathophysiology and for structure function studies of connexins.

MATERIALS AND METHODS

CHEMICALS AND REAGENTS

Clotrimazole (CAS No. 23593-75-1), triphenylmethane (CAS No. 519-73-3), triphenylmethyl chloride (CAS No. 76-83-5), triphenylmethanol (CAS No. 76-84-6), 3,3,3-triphenylpropionic acid (T51, CAS No. 900-91-4), (R)-(+)-α,α-diphenyl-2-pyrrolidinemethanol (T52, CAS No. 22348-32-9), (S)-(–)-α,α-diphenyl-2-pyrrolidinemethanol (T53, CAS No. 112068-01-6), diphenyl-4-pyridylmethane (T160, CAS No. 3678-72-6), and triphenylmethylamine (T162, CAS No. 5824-40-8) were purchased from Sigma-Aldrich (St. Louis, MO). Tetraphenylmethane (T161, CAS No. 630-76-2) was purchased from Alfa Aesar (Ward Hill, MA). 2-Chlorotriptyl chloride (T3-Cl, CAS No. 42074-68-0) and diphenyl-4-pyridylmethanol (T50, CAS No. 1620-30-0) were purchased from TCI America (Portland, OR). T1-T4, T9, T11, T13, T20, T34, T35, T39, T41, T43, T44, T54, T57, T61, T64, T66-T75, T78-T80, T85, and T97 were available in the Wulff laboratory compound library and had been previously synthesized and characterized (Wulff et al., 2000). The remaining compounds were synthesized using Grignard, chlorination and alkylation reactions described as general methods A, B, and C (see also **Figure 3**). New chemical entities (NCEs) were characterized by melting point (Melting Point B-540, Büchi), ¹H-NMR (Avance 500, Bruker), mass spectrometry (MS: LCQ, Thermo Scientific; HRMS: LTQ-Orbitrap XL Thermo Scientific), and/or combustion analysis (2400 Series II combustion analyzer, Perkin Elmer). All MS and HRMS spectra were recorded with ESI as ionization mode if not stated otherwise. In cases where no sufficient analytical data for

previously reported compounds (T109, T117, T129, T141, T143, T144, T154-OH, and T165) were available ¹H-NMR, MS and/or combustion data in addition to melting points are also provided.

CHEMICAL SYNTHESIS

General method A

Triaryl methanols were synthesized through a Grignard reaction by stirring 25 mmol of magnesium turnings and 10–15 mmol of the required arylbromide in 50 mL of anhydrous diethyl ether. To initiate the reaction, catalytic amounts of iodine were added. The remaining 15–20 mmol of the required arylbromide were diluted with or dissolved in anhydrous diethyl ether (50 mL) and added slowly allowing gentle reflux. The reaction mixture was refluxed until all magnesium was consumed. Then, a solution of the required benzophenone (25 mmol) in anhydrous diethyl ether (50 mL) was added drop wise and the resulting mixture was heated under reflux for 12–24 h. After completion of the reaction the mixture was cooled to 0°C, poured into 100 mL of cold water and acidified with concentrated HCl. The organic phase was separated, and the aqueous phase was extracted three times with diethyl ether. The organic phases were combined, washed with NaHCO₃ (10%) and dried over sodium sulfate. After evaporation of the solvent the crude triaryl methanols were obtained either as solid or as oily residues, which were recrystallized from petroleum ether (40–60°C) several times, if necessary.

General method B

The triaryl methyl chlorides were obtained according to McNaughton-Smith et al. (2008) by adding a five-fold excess of acetyl chloride to a stirred solution of the respective triaryl methanol in dichloromethane. After stirring the reaction mixture at room temperature for 12–24 h the solvent was evaporated and toluene (2 × 50 mL) was added and again removed under vacuum to afford the crude triaryl chlorides.

General method C

To a solution of the respective triaryl chloride (5 mmol) in anhydrous acetonitrile (100 mL) an excess of the respective amine (10–20 mmol) as hydrogen acceptor was added and the resulting mixture was refluxed for several hours. The progress of the reaction was monitored by TLC. Work up I: The mixture was poured into cold water (400 mL) and kept at 4°C for a few hours. The precipitate was filtered off, thoroughly washed with water to remove any remaining amine, and recrystallized from ethanol. Work up II: the solvent was evaporated and the crude residue was purified by column chromatography and/or recrystallization.

1-[(2-Chlorophenyl)(diphenyl)methyl]-4-methyl-2-phenyl-1H-imidazole (T89) was synthesized from T3-Cl (2.5 g, 7.98 mmol) and 4-methyl-2-phenylimidazole (1.26 g, 7.98 mmol), and triethylamine (1.11 ml, 7.98 mmol) as hydrogen acceptor in anhydrous acetonitrile (100 mL). After 24 h of refluxing the solvent was evaporated to afford a creamy residue, which was dissolved in dichloromethane (200 mL), washed with water (2 × 50 mL), and dried over Na₂SO₄. Evaporation of the solvent gave the crude product which was recrystallized from petroleum ether (40–60°C)/dichloromethane. T89 was obtained as a white powder (650 mg, 18.7%): Mp 226°C; ¹H NMR (DMSO-*d*₆) δ: 1.41 (s, 3H,

–CH₃), 6.92 (d, 1H, ³J = 6.9 Hz), 7.17–7.27 (m, 13H), 7.32 (dt, 1H, ³J = 7.3 Hz, ⁴J = 1.3 Hz), 7.39 (t, 2H, ³J = 7.7 Hz), 7.42 (d, 1H, ³J = 7.8 Hz), 7.83 (d, 2H, ³J = 7.5 Hz); MS (ESI) *m/z* calcd 435.2 [M + H]⁺; found 435.5 [M + H]⁺; Anal. calcd for C₂₉H₂₃ClN₂: C, 80.08; H, 5.33; N, 6.44; found: C, 79.70; H, 5.09; N, 6.59.

1-[(2-Chlorophenyl)diphenylmethyl]-2,5-dihydro-1*H*-pyrrole-2,5-dione (T91) was synthesized from T3-Cl (1.6 g, 5 mmol) and maleimide (1.94 g, 20 mmol) according to general method C as a slightly yellowish powder (320 mg, 17.12%): Mp 93°C; ¹H NMR (DMSO-*d*₆) δ: 6.43 (d, 1H, ³J = 1 Hz), 7.09 (dd, 1H, ³J = 7.8 Hz, ⁴J = 1.6 Hz), 7.22–7.27 (m, 8H), 7.29–7.32 (m, 5H), 7.39 (dd, 1H, ³J = 7.8 Hz, ⁴J = 1.3 Hz), MS (ESI) *m/z* calcd 338.1 [C₂₃H₁₆NO₂]⁺; found 338.2 [C₂₃H₁₆NO₂]⁺.

N-[(2-Chlorophenyl)diphenylmethyl]-*N*-(3-aminopropyl)imidazole (T94) was synthesized from T3-Cl (1.6 g, 5 mmol) and *N*-(3-aminopropyl)imidazole (1.88 g, 15 mmol) according to general method C as white powder (510 mg, 25.4%): Mp 89°C; ¹H NMR (DMSO-*d*₆) δ: 1.93–1.96 (m, 4H, 2x –CH₂), 2.84 (t, 1H, ³J = 7.6 Hz, *N*-H), 4.03 (t, 2H, ³J = 6.8 Hz, CH₂), 6.83 (s, 1H), 7.10 (s_{broad}, 1H), 7.14 (t, 2H, ³J = 7.3 Hz), 7.25 (t, 4H, ³J = 7.7 Hz), 7.31–7.35 (m, 2H), 7.37–7.39 (m, 5H), 7.53 (dd, 1H, ³J = 7.5 Hz, ⁴J = 2.0 Hz), 7.56 (s_{broad}, 1H); MS (ESI) *m/z* calcd 402.2 [M + H]⁺; found 402.3 [M + H]⁺; Anal. calcd for C₂₅H₂₄ClN₃: C, 74.71; H, 6.02; N, 10.45; found: C, 74.06; H, 6.44; N, 10.32.

N-[(2-Chlorophenyl)diphenylmethyl]-*N*-(3-aminopropionitrile)amine (T95) was synthesized from T3-Cl (1.6 g, 5 mmol) and 3-aminopropionitrile (1.12 mL, 1.05 g, 15 mmol) according to general method C as a white yellowish powder (610 mg, 35.2%): Mp 140°C; ¹H NMR (DMSO-*d*₆) δ: 2.13 (q, 2H, ³J = 7.1 Hz, NH-CH₂), 2.70 (t, 2H, ³J = 6.4 Hz, CH₂-CN), 3.19 (t, 1H, ³J = 8.4 Hz, *N*-H), 7.18 (t, 2H, ³J = 7.3 Hz), 7.29 (t, 4H, ³J = 7.7 Hz), 7.33–7.40 (m, 3H), 7.42–7.45 (m, 4H), 7.69 (d_{broad}, 1H, ³J = 7.7 Hz); HRMS (ESI) *m/z* calcd 347.1315 [M + H]⁺; found 347.1290 [M + H]⁺; Anal. calcd for C₂₂H₁₉ClN₂: C, 76.18; H, 5.52; N, 8.08; found: C, 75.53; H, 5.34; N, 8.06.

N-[(2-Chlorophenyl)diphenylmethyl]-3-(trifluoromethoxy)aniline (T102) was synthesized from T3-Cl (1.6 g, 5 mmol) and 3-(trifluoromethoxy)aniline (2.0 mL, 2.66 g, 15 mmol) according to general method C and recrystallized from methanol as white powder (1.34 g, 59%): Mp 144.2°C; ¹H NMR (CDCl₃) δ: 6.46 (d, 1H, ³J = 8 Hz), 6.49 (s, 1H, *N*-H), 6.67 (d, 1H, ³J = 8 Hz), 7.02 (t, 1H, ³J = 8.3 Hz), 7.11 (s, 1H), 7.32 (t, 2H, ³J = 7 Hz, phenyl-Cl-H4 and -H5), 7.36–7.46 (m, 11 H), 7.66 (d, 1H, ³J = 7 Hz); HRMS (ESI) *m/z* calcd 277.0784 [C₁₉H₁₄Cl]⁺, 178.0480 [C₇H₇NOF₃]⁺; found 277.0764 [C₁₉H₁₄Cl]⁺, 178.0461 [C₇H₇NOF₃]⁺; Anal. calcd for C₂₆H₁₉ClF₃NO: C, 68.80; H, 4.22; N, 3.09; found: C, 68.86; H, 4.02; N, 3.13.

N-[(2-Chlorophenyl)diphenylmethyl]-1,3-benzothiazol-2-amine (T103) was synthesized from T3-Cl (1.6 g, 5 mmol) and 2-aminobenzothiazole (2.25 g, 15 mmol) according to general method C and recrystallized from methanol as an off-white powder (1.12 g, 52%): Mp 156.3°C; ¹H NMR (DMSO-*d*₆) δ: 6.95 (t, 1H, ³J = 7.5 Hz), 7.00 (d, 1H, ³J = 8.5 Hz), 7.06 (t, 1H, ³J = 7.3 Hz), 7.20–7.23 (m, 2H), 7.28–7.31 (m, 11H), 7.49 (m, 1H), 7.60 (d, 1H, ³J = 7.5 Hz), 8.96 (s, 1H, *N*-H); HRMS (ESI) *m/z* calcd 427.1036 [M + H]⁺; found 427.1060 [M + H]⁺; Anal. calcd for

C₂₆H₁₉ClN₂S: C, 73.14; H, 4.49; N, 6.56; S, 7.51; found: C, 73.05; H, 4.39; N, 6.63; S, 8.07.

N-[(2-Chlorophenyl)diphenylmethyl]-2-(trifluoromethoxy)aniline (T104) was synthesized from T3-Cl (1.6 g, 5 mmol) and 2-trifluoromethoxyaniline (2.04 mL, 2.7 g, 15 mmol) according to general method C as a slightly yellowish powder (1.4 g, 62%): Mp 123.5°C; ¹H NMR (DMSO-*d*₆) δ: 5.91 (s, 1H, *N*-H), 6.12 (d, 1H, ³J = 7.8 Hz), 6.60 (dt, 1H, ³J = 8.2, Hz, ⁴J = 1.3 Hz), 6.57 (dt, 1H, ³J = 7.9 Hz, ⁴J = 1.3 Hz), 7.18–7.38 (m, 14H), 7.58 (d, 1H, ³J = 7.4 Hz); HRMS (ESI) *m/z* calcd 277.0784 [C₁₉H₁₄Cl]⁺, 178.0480 [C₇H₇NOF₃]⁺; found 277.0773 [C₁₉H₁₄Cl]⁺, 178.0465 [C₇H₇NOF₃]⁺; Anal. calcd for C₂₆H₁₉ClF₃NO: C, 68.8; H, 4.22; N, 3.09; found: C, 69.19; H, 4.26; N, 3.10.

1-(4-[(2-Chlorophenyl)diphenylmethyl]amino)phenyl)ethan-1-one (T105) was synthesized from T3-Cl (1.6 g, 5 mmol) and 4-aminoacetophenone (2.0 g, 15 mmol) according to general method C as a white powder (400 mg, 19.4%): Mp 166.7°C; ¹H NMR (DMSO-*d*₆) δ: 2.30 (s, 3H, –OCH₃), 6.55 (s_{wide}, 2H), 7.20–7.25 (m, 6H), 7.29–7.35 (m, 8H), 7.46 (d, 2H, ³J = 8.6 Hz), 7.56 (d, 1H, ³J = 7.4 Hz); HRMS (ESI) *m/z* calcd 412.1468 [M + H]⁺; found 412.1454 [M + H]⁺; Anal. calcd for C₂₇H₂₂ClNO: C, 78.73; H, 5.38; N, 3.40; found: C, 78.42; H, 5.48; N, 3.38.

N-[(2-Chlorophenyl)diphenylmethyl]-4-methoxyaniline (T106) was synthesized from T3-Cl (1.6 g, 5 mmol) and *p*-anisidine (1.85 g, 15 mmol) according to general method C and recrystallized from methanol as a slightly redish-beige powder (1.24 g, 62%): Mp 142.5°C; ¹H NMR (DMSO-*d*₆) δ: 3.52 (s, 3H, –OCH₃), 6.10 (s, 1H), 6.43 (s, 4H), 7.18 (t, 2H, ³J = 6 Hz), 7.26–7.30 (m, 11H), 7.59 (d, 1H, ³J = 7.5 Hz); HRMS (ESI) *m/z* calcd: 399.13899 [M]⁺; found: 399.1381 [M]⁺; Anal. calcd for C₂₆H₂₂ClNO: C, 78.09; H, 5.54; N, 3.50; found: C, 77.85; H, 5.62; N, 3.53.

1-Chloro-2-(phenoxydiphenylmethyl)benzene (T107): To a solution of T3-Cl (0.95 g, 3 mmol) in anhydrous acetone (50 mL) phenol (282 mg, 3 mmol), K₂CO₃ (1.93 g, 14 mmol) and catalytic amounts of KI were added. Afterward the resulting mixture was refluxed for several hours. The progress of the reaction was monitored by TLC. After completion of the reaction K₂CO₃ was filtered off and the solvent was evaporated. The solid residue was dissolved in CH₂Cl₂ and the solution was extracted three times with NaOH (0.5 M). The pooled organic phases were dried over Na₂SO₄ and concentrated *in vacuo*. The residue was recrystallized from ethanol to give an off-white, slightly yellowish powder (80 mg, 7%): Mp 125°C; ¹H NMR (DMSO-*d*) δ: 7.07 (dd, 2H, ³J = 8.1 Hz, ⁴J = 1.6 Hz), 7.12 (dt, 2H, ³J = 7.7 Hz, ⁴J = 1.4 Hz), 7.15–7.17 (m, 5H), 7.26 (dt, 2H, ³J = 7.6 Hz, ⁴J = 1.7 Hz), 7.29–7.31 (m, 8H); MS (FAB-NBA) *m/z* calcd 293 [C₁₉H₁₄ClO]⁺, 277 [C₁₉H₁₄Cl]⁺; found 293 [C₁₉H₁₄ClO]⁺, 277 [C₁₉H₁₄Cl]⁺.

N-[(2-Chlorophenyl)diphenylmethyl]aniline (T109) was synthesized from T3-Cl (0.95 g, 3 mmol) and aniline (279 mg, 3 mmol) as described for T107 and recrystallized from ethanol as a yellowish-beige powder (750 mg, 2 mmol, 67.6%): Mp 131.4°C (ethanol), Lit. 121°C (benzene; Gomberg and Van Slyke, 1911); ¹H NMR (DMSO-*d*₆) δ: 6.41–6.44 (m, 2H, *N*-H), 6.49 (d, 2H, ³J = 8.1 Hz), 6.80 (t, 2H, ³J = 7.8 Hz), 7.17–7.20 (m, 2H), 7.25–7.33 (m, 11H), 7.59 (d, 1H, ³J = 7.8 Hz); HRMS (ESI) *m/z* calcd 369.1284 [M]⁺; found 369.1277 [M]⁺.

2-[[2-(2-Chlorophenyl)diphenylmethyl]sulfanyl]pyrimidine (T112) was synthesized from T3-Cl (1.6 g, 5 mmol) and 2-mercaptopyrimidine (1.68 g, 15 mmol) according to general method C and recrystallized from methanol as an off-white powder (1.16 g, 60%): Mp 151.6°C; $^1\text{H NMR}$ (DMSO- d_6) δ : 7.00 (t, 1H, $^3J = 4.8$ Hz), 7.20 (t, 2H, $^3J = 7.2$ Hz), 7.26 (t, 4H, $^3J = 7.6$ Hz), 7.33–7.37 (m, 7H), 7.81–7.82 (m, 1H), 8.28 (d, 2H, $^3J = 4.9$ Hz); HRMS (ESI) m/z calcd 389.0879 $[\text{M} + \text{H}]^+$; found 389.0869 $[\text{M} + \text{H}]^+$; Anal. calcd for $\text{C}_{23}\text{H}_{17}\text{ClN}_2\text{S}$: C, 71.03; H, 4.41; N, 7.2; S, 8.24; found: C, 71.04; H, 4.26; N, 7.13; S, 8.56.

(2-Methoxyphenyl)diphenylmethanol (T117) was synthesized from 2-bromoanisole (3.09 mL, 4.68 g, 25 mmol) according to general method A as an off-white powder (4.9 g, 17 mmol, 67.6%): Mp 128.7°C; Lit. 128–129°C (Baeyer, 1907); $^1\text{H NMR}$ (DMSO- d_6) δ : 3.67 (s, 3H, -OCH₃), 5.28 (s, 1H, -OH), 6.54 (d, 1H, $^3J = 7.7$ Hz), 6.84 (t, 1H, $^3J = 7.6$ Hz), 6.97 (d, 1H, $^3J = 8.2$ Hz), 7.25–7.32 (m, 11H); HRMS (ESI) m/z calcd 273.12795 $[\text{M}-\text{OH}]^+$; found 273.1270 $[\text{M}-\text{OH}]^+$; Anal. calcd for $\text{C}_{20}\text{H}_{18}\text{O}_2$: C, 82.73; H, 6.25; found: C, 82.45; H, 6.20.

N-[(2-Methoxyphenyl)diphenylmethyl]-1,3-thiazol-2-amine (T122): In a first-step compound T117 was chlorinated with acetyl chloride according to method B to afford 1-(chlorodiphenylmethyl)-2-methoxybenzene (T117-Cl). Without further purification and characterization T117-Cl (3.7 g, 12 mmol) was reacted with 2-aminothiazole (2.9 g, 30 mmol) according to general method C to afford T122 as an off-white powder (1.67 g, 37%): Mp 162.3°C; $^1\text{H NMR}$ (DMSO- d_6) δ : 3.40 (s, 3H, -OCH₃), 6.49 (d, 1H, $^3J = 3.5$ Hz, thiazole-H4), 6.87 (d, 1H, $^3J = 3.3$, thiazole-H3), 6.89 (d, 1H, $^3J = 7.5$ Hz), 6.97 (d, 1H, $^3J = 8.1$ Hz), 7.12 (d, 1H, $^3J = 7.7$ Hz), 7.19–7.29 (m, 11H), 8.00 (s, 1H, *N*-H); HRMS (ESI) m/z calcd 373.1375 $[\text{M} + \text{H}]^+$; found 373.1371 $[\text{M} + \text{H}]^+$; Anal. calcd for $\text{C}_{23}\text{H}_{20}\text{N}_2\text{OS}$: C, 74.16; H, 5.41; N, 7.52; S, 8.61; found: C, 74.26; H, 5.31; N, 7.29; S, 8.87.

N-[(2-Methoxyphenyl)diphenylmethyl]pyrimidin-2-amine (T123): T117 was chlorinated to afford T117-Cl as described for T122. In a next step T117-Cl (6.48 g, 21 mmol) and 2-aminopyrimidine (5.02 g, 52.75 mmol) were reacted according to general method C to give T123 as an off-white powder (2.15 g, 27.9%): Mp 166.5°C; $^1\text{H NMR}$ (CD₃COCD₃) δ : 3.44 (s, 3H, -OCH₃), 6.48 (t, 1H, $^3J = 4.8$ Hz), 6.83–6.86 (m, 2H, *N*-H), 6.92 (d, 1H, $^3J = 7.8$ Hz), 7.14–7.16 (m, 2H), 7.20–7.26 (m, 6H), 7.29–7.31 (m, 4H) 8.02 (s, 2H); HRMS (ESI) m/z calcd 368.1763 $[\text{M} + \text{H}]^+$; found 368.1757 $[\text{M} + \text{H}]^+$; Anal. calcd for $\text{C}_{24}\text{H}_{21}\text{N}_3\text{O}$: C, 78.45; H, 5.76; N, 11.44; found: C, 78.37; H, 5.71; N, 11.18.

N-[(2-Methylphenyl)diphenylmethyl]-1,3-thiazol-2-amine (T124): (2-Methylphenyl)diphenylmethanol (T118) was synthesized from 1-bromo-2-methylbenzene (3.01 mL, 4.28 g, 25 mmol) according to general method A and then chlorinated according to method B to afford 1-(chlorodiphenylmethyl)-2-methylbenzene (T118-Cl). Without further purification and characterization T118-Cl (2.9 g, 9.9 mmol) was immediately reacted with 2-aminothiazole (2.48 g, 24.8 mmol) according to general method C. T124 was obtained as a beige powder after recrystallization from ethanol (2.69 g, 76%): Mp 158.3°C; $^1\text{H NMR}$ (CDCl₃) δ : 1.97 (s, 3H, phenyl-CH₃), 6.26 (d, 1H, $^3J = 4$ Hz, thiazole-H4), 6.86 (s, 1H, *N*-H), 7.04 (d, 1H, $^3J = 4$ Hz, thiazole-H3), 7.12 (d, 2H, $^3J = 8$ Hz), 7.20–7.27 (m, 12H); HRMS (ESI) m/z calcd 357.1426

$[\text{M} + \text{H}]^+$, 373.1375 $[\text{M} + \text{H}_2\text{O}]^+$; found 357.1420 $[\text{M} + 1]^+$, 373.1357 $[\text{M} + \text{H}_2\text{O}]^+$; Anal. calcd for $\text{C}_{23}\text{H}_{20}\text{N}_2\text{S}$: C, 77.49; H, 5.65; N, 7.86; S, 8.99; found: C, 76.87; H, 5.67; N, 7.7; S, 9.48.

N-[(2-Methylphenyl)diphenylmethyl]-pyrimidin-2-amine (T125): (2-Methylphenyl)diphenylmethanol (T118) was synthesized and afterward chlorinated (T118-Cl) as described for T124. Without further purification and characterization T118-Cl (2.9 g, 9.9 mmol) was immediately reacted with 2-aminopyrimidine (2.36 g, 24.8 mmol) according to general method C. T125 was obtained as a white powder after recrystallization from ethanol (1.46 g, 42%): Mp 183.1°C; $^1\text{H NMR}$ (CDCl₃) δ : 1.99 (s, 3H, phenyl-CH₃), 6.43 (t, 1H, $^3J = 4.8$ Hz, pyrimidine-H5), 7.05 (d, 1H, $^3J = 7.1$ Hz), 7.08 (d, 1H, $^3J = 7.7$ Hz), 7.14–7.29 (m, 14H), 8.05 (s_{broad}, 2H); HRMS (ESI) m/z calcd 352.1814 $[\text{M} + \text{H}]^+$; found 352.1808 $[\text{M} + \text{H}]^+$; Anal. calcd for $\text{C}_{24}\text{H}_{21}\text{N}_3$: C, 82.02; H, 6.02; N, 11.96; found: C, 81.79; H, 5.93; N, 11.86.

N-[Diphenyl[2-(trifluoromethoxy)phenyl]methyl]-1,3-thiazol-2-amine (T126): Diphenyl[2-(trifluoromethoxy)phenyl]methanol (T119) was synthesized from 1-bromo-2-(trifluoromethoxy)benzene (3.69 mL, 6.03 g, 25 mmol) according to general method A. Without further purification and characterization T119 was chlorinated according to method B to afford 1-(chlorodiphenylmethyl)-2-(trifluoromethoxy)benzene (T119-Cl). Without further purification and characterization T119-Cl (g, 14.38 mmol) was immediately reacted with 2-aminothiazole (3.6 g, 35.94 mmol) according to general method C. T126 was obtained as an off-white powder after recrystallization from ethanol (2.25 g, 36.7%): Mp 178.8°C; $^1\text{H NMR}$ (CDCl₃) δ : 6.24 (d, 1H, $^3J = 3.6$ Hz, thiazole-H4), 6.82 (s, 1H, *N*-H), 6.98 (d, 1H, $^3J = 3.6$ Hz, thiazole-H3), 7.10–7.29 (m, 13H), 7.41 (dd, 1H, $^3J = 8.1$ Hz, $^4J = 1.4$ Hz); HRMS (ESI) m/z calcd 427.1092 $[\text{M} + \text{H}]^+$; found 427.1087 $[\text{M} + \text{H}]^+$; Anal. calcd for $\text{C}_{23}\text{H}_{17}\text{F}_3\text{N}_2\text{OS}$: C, 64.78; H, 4.02; N, 6.57; S, 7.52; found: C, 64.64; H, 3.89; N, 6.56; S, 8.1.

N-[Diphenyl[2-(trifluoromethoxy)phenyl]methyl]pyrimidin-2-amine (T127): Diphenyl[2-(trifluoromethoxy)phenyl]methanol (T119) was synthesized and afterward chlorinated (T119-Cl) as described for T126. Without further purification and characterization T119-Cl (5.2 g, 14.38 mmol) and 2-aminopyrimidine (3.42 g, 35.94 mmol) were reacted according to general method C. T127 was obtained as a white powder after recrystallization from ethanol (1.2 g, 19.8%): Mp 135°C; $^1\text{H NMR}$ (DMSO- d_6) δ : 6.54 (t, 1H, $^3J = 4.8$ Hz, pyrimidine-H4), 7.00 (s, 1H, *N*-H), 7.15–7.20 (m, 3H), 7.24–7.29 (m, 9H), 7.39 (ddd, 1H, $^3J = 8.2$ Hz, $^3J = 7.4$ Hz, $^4J = 1.7$ Hz), 7.51 (dd, 1H, $^3J = 8$ Hz, $^4J = 1.7$ Hz), 8.07 (s_{broad}, 2H, pyrimidine-H3 and -H5); HRMS (ESI) m/z calcd 422.1480 $[\text{M} + \text{H}]^+$; found 422.1471 $[\text{M} + \text{H}]^+$; Anal. calcd for $\text{C}_{24}\text{H}_{18}\text{F}_3\text{N}_3\text{O}$: C, 68.4; H, 4.31; N, 9.97; found: C, 68.3; H, 4.58; N, 9.99.

N-[(2-Fluorophenyl)diphenylmethyl]pyrimidine-2-amine (T128): (2-Fluorophenyl)diphenylmethanol (T36) was synthesized from bromobenzene (2.63 mL, 3.93 g, 25 mmol) and 2-fluorobenzophenone (4.22 mL, 5.0 g, 25 mmol) according to general method A (yellowish solid, 6.5 g, 93.41%). Spectroscopic data were in accordance with literature (Wulff et al., 2000). In a next step T36 was chlorinated according to method B to afford 1-(chlorodiphenylmethyl)-2-fluorobenzene (T36-Cl).

Without further purification and characterization T36-Cl (3 g, 10.28 mmol) was immediately reacted with 2-aminopyrimidine (2.44 g, 25.7 mmol) according to general method C. T128 was obtained as slightly yellowish powder after recrystallization from ethanol (1.73 g, 47.3%): Mp 161.1°C; ^1H NMR (DMSO- d_6) δ : 6.53 (t, 1H, $^3J = 5$ Hz, pyrimidine-H4), 7.01 (dd, 1H, $^3J = 12$ Hz, $^3J = 8$ Hz), 7.11 (t, 1H, $^3J = 7.9$ Hz), 7.18 (t, 2H, $^3J = 6.4$ Hz), 7.23–7.30 (m, 9H), 7.34 (s, 1H, *N*-H), 7.40 (dt, 1H, $^3J = 8$ Hz, $^4J = 1.3$ Hz), 8.07 (s_{broad} , 2H, pyrimidine-H3 and -H5); HRMS (ESI) m/z calcd: 356.1563 $[\text{M} + \text{H}]^+$; found: 356.1563 $[\text{M} + \text{H}]^+$; Anal. calcd for $\text{C}_{23}\text{H}_{18}\text{FN}_3$: C, 77.73; H, 5.10; N, 11.82; found: C, 77.55; H, 4.95; N, 11.42.

N-[(3-Chlorophenyl)diphenylmethyl]-1,3-thiazol-2-amine (T129): (3-Chlorophenyl)diphenylmethanol (T2) was synthesized from 1-bromo-3-chlorobenzene (2.94 mL, 4.79 g, 25 mmol) according to general method A (5.0 g, 67.8%). Spectroscopic data were in accordance with literature (Wulff et al., 2000). T2 was then chlorinated according to general method B to afford 1-chloro-3-(chlorodiphenylmethyl)benzene (T2-Cl). Without further purification and characterization T2-Cl (2.75 g, 8.78 mmol) was reacted with 2-aminothiazole (2.2 g, 21.95 mmol) according to general method C. T129 was obtained as a beige powder after recrystallization from ethanol (3.0 g, 91%): Mp 164.5°C; ^1H NMR (DMSO- d_6) δ : 6.56 (d, 1H, $^3J = 3.6$ Hz, thiazole-H4), 6.81 (d, 1H, $^3J = 3.7$ Hz, thiazole-H3), 7.18–7.31 (m, 13H), 7.35 (t, 1H, $^3J = 1.8$ Hz), 8.57 (s, 1H, *N*-H); HRMS (ESI) m/z calcd 377.0879 $[\text{M} + \text{H}]^+$; found 377.0861 $[\text{M} + \text{H}]^+$; Anal. calcd for $\text{C}_{22}\text{H}_{17}\text{ClN}_2\text{S}$: C, 70.11; H, 4.55; N, 7.43; S, 8.51; found: C, 69.94; H, 4.46; N, 7.48; S, 9.09.

N-[(3-Chlorophenyl)diphenylmethyl]pyrimidin-2-amine (T130): (3-Chlorophenyl)diphenylmethanol (T2) was synthesized and afterward chlorinated (T2-Cl) as described for T129. Without further purification and characterization T2-Cl (2.75 g, 8.78 mmol) and 2-aminopyrimidine (2.1 g, 21.95 mmol) were reacted according to general method C. T130 was obtained as a white powder after recrystallization from ethanol (1.65 g, 51%): Mp 124.4°C; ^1H NMR (DMSO- d_6) δ : 6.53 (t, 1H, $^3J = 4.8$ Hz, pyrimidine-H4), 7.16 (t, 2H, $^3J = 7.2$ Hz), 7.22–7.28 (m, 7H), 7.30–7.32 (m, 4H), 7.35 (s_{broad} , 1H), 7.87 (s, 1H, *N*-H), 8.10 (d, 2H, $^3J = 4.3$ Hz, pyrimidine-H3 and -H5); HRMS (ESI) m/z calcd 372.1262 $[\text{M} + \text{H}]^+$; found 372.1253 $[\text{M} + \text{H}]^+$; Anal. calcd for $\text{C}_{23}\text{H}_{18}\text{ClN}_3$: C, 74.29; H, 4.88; N, 11.3; found: C, 74.14; H, 4.76; N, 11.21.

N-[(2-Bromophenyl)diphenylmethyl]-1,3-thiazol-2-amine (T131): (2-Bromophenyl)diphenylmethanol (T116) was synthesized according to method A (bromobenzene (2.84 mL, 4.24 g, 27 mmol) and 2-bromobenzophenone (6.52 g, 25 mmol). The crude oily T116 was chlorinated in a next step according to method B to afford 1-bromo-2-(chlorodiphenylmethyl)benzene (T116-Cl). Without further purification and characterization T116-Cl was immediately reacted with 2-aminothiazole (6.3 g, 62.5 mmol) according to general method C. T131 was obtained as white powder [silica column: cyclohexane/ethylacetate (8/2); 1.05 g, 10%]: Mp 142°C; ^1H NMR (DMSO- d_6) δ : 6.52 (d, 1H, $^3J = 3.7$ Hz, thiazole-H4), 6.74 (d, 1H, $^3J = 3.6$ Hz, thiazole-H3), 7.17–7.20 (m, 3H), 7.28 (m, 7H), 7.32–7.29 (m, 2H), 7.41 (dd, 1H, $^3J = 8$ Hz, $^4J = 1.4$ Hz), 7.52 (d, 1H, $^3J = 7.8$ Hz) 8.36 (s, 1H, *N*-H); HRMS

(ESI) m/z calcd 421.0374 $[\text{M} + \text{H}]^+$, 423.0353, found 421.0366 $[\text{M} + \text{H}]^+$, 423.0335.

N-[(2-Bromophenyl)diphenylmethyl]-pyrimidin-2-amine (T132): (2-Bromophenyl)diphenylmethanol (T116) was synthesized and afterward chlorinated (T116-Cl) as described for T131. T116-Cl (4.5 g, 12.5 mmol) was immediately without further purification and characterization reacted with 2-aminopyrimidine (1.2 g, 12.6 mmol) according to general method C. T132 was obtained as an off-white to yellowish powder after recrystallization from ethanol (850 mg, 16%): Mp 158.7°C; ^1H NMR (DMSO- d_6) δ : 6.57 (t, 1H, $^3J = 4.5$ Hz, pyrimidine-H4), 7.10 (s, 1H), 7.14–7.32 (m, 13H), 7.49 (d, 2H, $^3J = 8.5$ Hz, pyrimidine-H3 and -H5), 8.10 (s, 1H, *N*-H); HRMS (ESI) m/z calcd 416.0762 $[\text{M} + \text{H}]^+$, 418.0742, 419.0776; found 416.0758 $[\text{M} + \text{H}]^+$, 418.0728, 419.0752; Anal. calcd for $\text{C}_{23}\text{H}_{18}\text{BrN}_3$: C, 66.36; H, 4.36; N, 10.09; found: C, 66.16; H, 4.23; N, 9.74.

N-{diphenyl[3-(trifluoromethyl)phenyl]methyl}-1,3-thiazol-2-amine (T133): Diphenyl[3-(trifluoromethoxy)phenyl]methanol (T121) was synthesized from 1-bromo-3-(trifluoromethoxy)benzene (3.49 mL, 5.63 g, 25 mmol) and benzophenone (4.56 g, 25 mmol) according to general method A. T121 was then chlorinated according to method B to afford 1-(chlorodiphenylmethyl)-3-(trifluoromethoxy)benzene (T121-Cl). Without further purification and characterization T121-Cl (4.5 g, 12.98 mmol) was immediately reacted with 2-aminothiazole (3.25 g, 32 mmol) according to general method C. T133 was obtained as a white powder after recrystallization from ethanol (3.64 g, 68%): Mp 120.5°C; ^1H NMR (DMSO- d_6) δ : 6.56 (d, 1H, $^3J = 3.7$ Hz, thiazole-H4), 6.79 (d, 1H, $^3J = 3.7$ Hz, thiazole-H3), 7.19–7.22 (m, 2H), 7.27–7.32 (m, 8H), 7.50 (t, 1H, $^3J = 8.1$ Hz), 7.57 (t, 2H, $^3J = 9.1$ Hz), 7.67 (s, 1H), 8.64 (s, 1H, *N*-H); HRMS (ESI) m/z calcd 411.1137 $[\text{M} + \text{H}]^+$; found 411.1137 $[\text{M} + \text{H}]^+$; Anal. calcd for $\text{C}_{23}\text{H}_{17}\text{F}_3\text{N}_2\text{S}$: C, 67.3; H, 4.17; N, 6.82; S, 7.81; found: C, 67.39; H, 3.98; N, 6.85; S, 7.82.

N-{Diphenyl[3-(trifluoromethyl)phenyl]methyl}pyrimidin-2-amine (T134): Diphenyl[3-(trifluoromethoxy)phenyl]methanol (T121) was synthesized and afterward chlorinated (T121-Cl) as described for T133. In a next step T121-Cl (4.5 g, 12.98 mmol) was immediately reacted with 2-aminopyrimidine (3.1 g, 32.4 mmol) according to general method C. T134 was obtained as an off-white powder after recrystallization from ethanol (1.95 g, 37%): Mp 161.4°C; ^1H NMR (DMSO- d_6) δ : 6.53 (t, 1H, $^3J = 4.8$ Hz, pyrimidine-H4), 7.17 (t, 2H, $^3J = 7.18$ Hz, 2 \times phenyl-H4), 7.25 (t, 4H, $^3J = 7.7$ Hz, 2 \times phenyl-H3 and -H5), 7.31 (d, 4H, $^3J = 7.7$ Hz, 2 \times phenyl-H2 and -H6), 7.48 (t, 1H, $^3J = 7.8$ Hz, phenyl-CF₃-H5), 7.53 (d, 1H, $^3J = 7.8$ Hz, phenyl-CF₃-H6), 7.62 (d, 1H, $^3J = 7.9$ Hz, phenyl-CF₃-H4), 7.67 (s_{wide} , 1H, phenyl-CF₃-H2), 8.00 (s, 1H, *N*-H), 8.09 (d, 2H, $^3J = 4$ Hz, pyrimidine-H3 and -H5); HRMS (ESI) m/z calcd 406.1526 $[\text{M} + \text{H}]^+$, found 406.1521 $[\text{M} + \text{H}]^+$, Anal. calcd for $\text{C}_{24}\text{H}_{18}\text{F}_3\text{N}_3$: C, 71.1; H, 4.48; N, 10.36; found: C, 71.03; H, 4.29; N, 10.26.

N-[(2-Iodophenyl)diphenylmethyl]-1,3-thiazol-2-amine (T136): (2-Iodophenyl)diphenylmethanol (T135) was synthesized according to general method A from bromobenzene (2.1 mL, 3.13 g, 20 mmol) and 2-iodobenzophenone (6 g, 19.5 mmol). The crude oily T135 was then chlorinated according to method B to afford 1-(chlorodiphenylmethyl)-2-iodobenzene (T135-Cl).

Without further purification and characterization T135-Cl was immediately reacted with 2-aminothiazole (1.5 g, 15 mmol) according to general method C. T136 was obtained as a slightly yellowish powder (silica column cyclohexane/ethylacetate (8/2); 80 mg, 2.8%): Mp 81°C; ¹H NMR (DMSO-*d*₆) δ: 6.52 (d, 1H, ³J = 2.6 Hz, thiazole-H4), 6.78 (d, 1H, ³J = 2.6 Hz, thiazole-H3), 6.96–6.98 (m, 1H), 7.20–7.32 (m, 12H), 7.88 (d, 1H, ³J = 7.6 Hz, phenyl-I-H3), 8.25 (s, 1H, *N*-H); HRMS (ESI) *m/z* calcd: 469.0236 [M + H]⁺; found: 469.0213 [M + H]⁺.

N-[(2-Iodophenyl)diphenylmethyl]-pyrimidin-2-amine (T137): (2-Iodophenyl)diphenyl methanol (T135) was synthesized and afterward chlorinated (T135-Cl) as described for T136. In a next step T135-Cl (2.4 g, 6 mmol) was immediately without further purification and characterization reacted with 2-aminopyrimidine (1.43 g, 15 mmol) according to general method C. T137 was obtained as an off-white to yellowish powder [silica column cyclohexane/ethylacetate (8/2); 570 mg, 20.5%]: Mp 160.7°C; ¹H NMR (DMSO-*d*₆) δ: 6.58 (dt, 1H, ³J = 4.7 Hz, ⁴J = 1.2 Hz), 6.93 (t, 1H, ³J = 7.5 Hz), 7.05 (s_{broad}, 1H), 7.19–7.32 (m, 11H), 7.44 (d, 1H, ³J = 8 Hz), 7.82 (d, 1H, ³J = 7.8 Hz), 8.1 (s_{broad}, 2H, pyrimidine-H3 and -H5); MS (ESI) *m/z* calcd 469.4 [M + H]⁺; found 496.3 [M + H]⁺; Anal. calcd for C₂₃H₁₈IN₃: C, 59.62; H, 3.92; N, 9.07; found: C, 60.38; H, 3.74; N, 8.84.

N-(Triphenylmethyl)pyrimidin-2-amine (T141) was synthesized from (chlorophenylmethyl)benzene (1.34 g, 4.82 mmol) and 2-aminopyrimidine (1.48 g, 15.56 mmol) according to general method C as a white powder (1.18 g, 72.4%): Mp 174.2°C; Lit. 174–175°C (Dahlbom and Ekstrand, 1944). Spectroscopic data were in accordance with literature (Zunszain et al., 2002).

1-[(3-Chlorophenyl)diphenylmethyl]-1*H*-pyrazole (T142): (3-Chlorophenyl)diphenylmethanol (T2) was synthesized and afterward chlorinated (T2-Cl) as described for T129. Without further purification and characterization T2-Cl (3.3 g, 10.54 mmol) and pyrazole (1.77 g, 26 mmol) were reacted according to general method C. T142 was obtained as a white powder after recrystallization from ethanol (3.1 g, 85.3%): Mp 127.3°C; ¹H NMR (DMSO-*d*₆) δ: 6.33 (t, 1H, ³J = 2.1 Hz), 6.99–7.04 (m, 5H), 7.10 (t, 1H, ³J = 1.9 Hz), 7.34–7.43 (m, 9H), 7.66 (d, 1H, ³J = 1.6 Hz); HRMS (ESI) *m/z* calcd 69.04528 [C₃H₅N₂]⁺, 277.0784 [C₁₉H₁₄Cl]⁺, found 69.0432 [C₃H₅N₂]⁺, 277.0757 [C₁₉H₁₄Cl]⁺; Anal. calcd for C₂₂H₁₇ClN₂: C, 76.63; H, 4.97; N, 8.12; found: C, 76.13; H, 4.92; N, 8.13.

1-[(3-Chlorophenyl)diphenylmethyl]-1*H*-imidazole (T143): (3-Chlorophenyl)diphenylmethanol (T2) was synthesized and afterward chlorinated (T2-Cl) as described for T129. Without further purification and characterization T2-Cl (3.3 g, 10.54 mmol) and imidazole (1.77 g, 26 mmol) were reacted according to general method C. T143 was obtained as a white powder after recrystallization from ethanol (1.3 g, 35.77%): Mp 121.3°C, Lit. 122–124°C (Bartroli et al., 1992); ¹H NMR (DMSO-*d*₆) δ: 6.94 (s_{broad}, 1H, imidazole-H5), 7.01 (s_{broad}, 1H, imidazole-H4), 7.03–7.04 (m, 2H), 7.06 (td, 1H, ³J = 6.8 Hz, ⁴J = 2.1 Hz), 7.09–7.1 (m, 3H), 7.36–7.47 (m, 9H), 8.46 (s, 1H, imidazole-H2); HRMS (ESI) *m/z* calcd for C₂₂H₁₇ClN₂ 345.1159 [M + H]⁺, found 345.1148 [M + H]⁺.

1-[(4-Chlorophenyl)diphenylmethyl]-1*H*-imidazole (T144): (4-Chlorophenyl)diphenylmethanol (T1) was synthesized from

magnesium turnings (1.2 g, 50 mmol), 1-bromo-4-chlorobenzene (11.5 g, 60 mmol) and benzophenone (9.12 g, 50 mmol) according to general method A. Spectroscopic data were in accordance with literature (Wulff et al., 2000). The crude T1 was chlorinated according to method B to afford 1-chloro-4-(chlorodiphenylmethyl)benzene (T1-Cl). Without further purification and characterization T1-Cl (~8 g, 25.5 mmol) was immediately reacted with imidazole (4.34 g, 63.75 mmol) according to general method C. T144 was obtained as a white powder (0.6 g, 3.5%): Mp 141.2°C, Lit. 140–142°C (Bartroli et al., 1992); ¹H NMR (DMSO-*d*₆) δ: 6.90 (s_{broad}, 1H), 6.99 (s_{broad}, 1H), 7.07–7.09 (m, 6H), 7.36 (m, 7H), 7.47 (d, 2H, ³J = 8.7 Hz); HRMS (ESI) *m/z* calcd for C₂₂H₁₇ClN₂ 345.1159 [M + H]⁺, found 345.1126 [M + H]⁺.

N-[(4-Chlorophenyl)diphenylmethyl]pyrimidin-2-amine (T145): (4-Chlorophenyl)diphenylmethanol (T1) was synthesized and afterward chlorinated (T1-Cl) as described for T144. Without further purification and characterization T1-Cl (15.7 g, 50 mmol) was reacted with 2-aminopyrimidine (11.88 g, 128 mmol) according to general method C. T145 was obtained as a white powder after recrystallization from ethanol (2.3 g, 12%): Mp 117.8°C; ¹H NMR (DMSO-*d*₆) δ: 6.51–6.54 (m, 3H, pyrimidine-H4), 7.15 (t, 2H, ³J = 7.2 Hz), 7.24 (t, 3H, ³J = 7.7 Hz), 7.28–7.34 (m, 6H), 7.80 (s, 1H, *N*-H), 8.09 (d, 2H, ³J = 3.5 Hz, pyrimidine-H3 and -H5), 8.19 (d, 2H, ³J = 4.8 Hz); HRMS (ESI) *m/z* calcd 372.1268 [M + H]⁺, found 372.1261 [M + H]⁺.

N-[(2-Chlorophenyl)diphenylmethyl]-4-(trifluoromethoxy)aniline (T150) was synthesized from T3-Cl (1.6 g, 5 mmol) and 4-(trifluoromethoxy)aniline (2.01 mL, 2.66 g, 15 mmol) according to general method C and recrystallized from ethanol as an off-white powder (1.5 g, 66%): Mp 99°C; ¹H NMR (DMSO-*d*₆) δ: 6.54 (d, 2H, ³J = 8.9 Hz), 6.82–6.80 (m, 3H, *N*-H), 7.18–7.22 (m, 2H), 7.26–7.36 (m, 11H), 7.58 (d, 1H, ³J = 7.9 Hz, phenyl-Cl-H3); HRMS (ESI) *m/z* calcd 454.1180 [M + H]⁺, 178.0474 [C₇H₆F₃NO + H]⁺, found 454.1156 [M + H]⁺, 178.0461 [C₇H₆F₃NO + H]⁺; Anal. calcd for C₂₆H₁₉ClF₃NO: C, 68.8; H, 4.22; N, 3.09; found: C, 68.52; H, 4.09; N, 3.05.

(2-Aminophenyl)diphenylmethanol (T154-OH) was synthesized from phenylmagnesium bromide (1.89 g, 15.3 mmol) and 2-aminobenzophenone (2 g, 10.2 mmol) according to general method A (125 mg, 4.5%) as a red crystalline solid: Mp 117.4–118.9°C; Lit. 116–117°C (Misra et al., 1983); ¹H NMR (DMSO-*d*₆) δ: 5.07 (s, 2H, -NH₂), 6.23 (d, 1H, ³J = 7.8 Hz), 6.34 (t, 1H, ³J = 7.4 Hz), 6.60 (d, 1H, ³J = 8.0 Hz), 6.73 (s, 1H, -OH), 7.31–7.17 (m, 10H); MS (ESI) *m/z* calcd 258.13 [C₁₉H₁₆N]⁺, 180.1 [C₁₃H₁₀N]⁺, found 258.3 [C₁₉H₁₆N]⁺, 180.1 [C₁₃H₁₀N]⁺; Anal. calcd for C₁₉H₁₇NO: C, 82.88; H, 6.22; N, 5.09; found: C, 82.42; H, 6.09; N, 5.17.

Bis-(2-methoxyphenyl)(phenyl)methanol (T165) was synthesized from magnesium turnings (0.6 g, 25 mmol), 1-bromo-2-methoxybenzene (4.0 mL, 5.99 g, 32 mmol) and 2-methoxybenzophenone (5.0 g, 23.5 mmol) according to general method A and recrystallized from ethanol as a white powder (1.2 g, 15.8%): Mp 115.8°C; Lit. 115°C (Baeyer, 1907); ¹H NMR (DMSO-*d*₆) δ: 3.39 (s, 6H, -OCH₃), 5.37 (s, 1H, -OH), 6.87 (dt, 2H, ³J = 7.3 Hz, ⁴J = 0.7 Hz), 6.98 (d, 2H, ³J = 7.9 Hz), 7.03 (dd,

2H, $^3J = 7.8$ Hz, $^3J = 1.5$ Hz), 7.15–7.17 (m, 3H), 7.20–7.21 (m, 2H) 7.23–7.27 (m, 2H); MS (ESI) m/z calcd 343.38 [M + Na⁺], 303.14 [M-OH]⁺, found 343.1 [M + Na⁺], 303.1 [M-OH]⁺; Anal. calcd for C₂₁H₂₀O₃: C, 78.73; H, 6.29; found: C, 78.14; H, 6.97.

N-[bis(2-methoxyphenyl)(phenyl)methyl]-1,3-thiazol-2-amine (T166): In a first-step T165 was chlorinated according to general method B (T165-Cl). The crude T165-Cl (530 mg, 1.56 mmol) was immediately reacted with 2-aminothiazole (392 mg, 3.9 mmol) according to general method C. After recrystallization from ethanol T166 was obtained as a white powder (250 mg, 39.8%): Mp 150°C; ¹H NMR (DMSO-*d*₆) δ: 3.39 (s, 6H, -OCH₃), 6.44 (d, 1H, $^3J = 3.6$ Hz), 6.88 (dt, 2H, $^3J = 7.8$ Hz, $^4J = 1.0$ Hz), 6.90 (d, 1H, $^3J = 3.6$ Hz), 6.95 (d, 2H, $^3J = 8.2$ Hz), 7.08 (d, 2H, $^3J = 7.6$ Hz), 7.16 (d, 2H, $^3J = 7.1$ Hz), 7.21–7.29 (m, 5H), 7.81 (s, 1H); HRMS (ESI) m/z calcd for C₂₄H₂₂N₂O₂S 403.1480 [M + H]⁺, found 403.1465 [M + H]⁺.

CELLS AND CLONES

All electrophysiological experiments described here were performed on N2A neuroblastoma cells that were transiently cotransfected with connexin and enhanced green fluorescent protein cDNAs as described previously (Srinivas et al., 2001). The connexins used in the study were rCx26, rCx32, rCx43, rCx46, and mCx50 (where r and m refer to rat, and mouse cDNAs, respectively). Transiently transfected cells were dissociated at 8–12 h after transfection, plated at low density on 1 cm round glass coverslips, and used within 48 h thereafter.

HEK-293 cells stably expressing hKCa3.1 were obtained from Khaled Houamed, University of Chicago, IL. The cloning of hKCa2.3 (19 CAG repeats) and hKCa3.1 has been previously described (Wulff et al., 2001). The hKCa2.3 clone was later stably expressed in COS-7 cells at Aurora Biosciences Corp., San Diego, CA. Cell lines stably expressing other mammalian ion channels were gifts from several sources: hKCa1.1 in HEK-293 cells (Andrew Tinker, University College London); rKv4.2 in LTK cells (Michael Tamkun, University of Colorado, Boulder); Kv11.1 (HERG) in HEK-293 cells (Craig January, University of Wisconsin, Madison); hNav1.4 in HEK-293 cells (Frank Lehmann-Horn, University of Ulm, Germany) and Cav1.2 in HEK-293 cells (Franz Hofmann, Munich, Germany). Cells stably expressing mKv1.1, mKv1.3, hKv1.5, and mKv3.1 have been previously described (Grissmer et al., 1994); N1E-115 neuroblastoma cells (expressing Nav1.2) were obtained from ATCC. Rat Nav1.5 in pSP64T was provided by Roland G. Kallen (University of Pennsylvania), inserted into pcDNA-3.1(+) as described (Sankaranarayanan et al., 2009), and transiently transfected into COS-7 cells together with eGFP-C1 with Fugene-6 (Roche) according to the manufacturer's protocol. Human Kv7.2 and Kv7.3 in PTLN or pcDNA-3 was provided by Bernhard Attali (Weizmann Institute of Science, Rehovot, Israel).

ELECTROPHYSIOLOGY

Junctional current measurements were performed on N2A neuroblastoma cells transiently transfected with cDNAs corresponding to individual connexins or on mouse primary lens epithelial cells isolated from postnatal day 6. Dissociation of lens epithelial was performed as described previously (White et al., 2007).

Junctional conductance was measured between cell pairs using the dual whole-cell voltage-clamp technique with Axopatch 1D patch-clamp amplifiers (Molecular Devices, CA) at room temperature. Each cell of a pair was initially held at a common holding potential of 0 mV. To evaluate junctional coupling, 200 msec hyperpolarizing pulses from the holding potential of 0 mV to -20 mV were applied to one cell to establish a transjunctional voltage gradient (V_j), and junctional current was measured in the second cell (held at 0 mV). The solution bathing the cells contained 140 mM NaCl, 5 mM KCl, 2 mM CsCl, 2 mM CaCl₂, 1 mM MgCl₂, 5 mM HEPES, 5 mM dextrose, 2 mM pyruvate, and 1 mM BaCl₂, pH 7.4. Patch electrodes had resistances of 3–5 MΩ when filled with internal solution containing 130 mM CsCl, 10 mM EGTA, 0.5 mM CaCl₂, 3 mM MgATP, 2 mM Na₂ATP, and 10 mM HEPES, pH 7.2. Macroscopic recordings were filtered at 0.2–0.5 kHz and sampled at 1–2 kHz. Data were acquired using pClamp software (Axon Instruments) and plotted using Origin 6.0 software (OriginLab Corp, Northampton, MA). Drugs were applied with a gravity-fed perfusion system. Solution exchanges were complete within 10–20 s. All compounds were applied to Cx50 expressing N2A cells at an initial concentration of 10 μM. Compounds that reduced Cx50 junctional currents by >80% at 10 μM were then applied at lower concentrations ranging from 0.5 to 5 μM. Concentration-response curves for drug-induced uncoupling were typically determined by exposure of each cell pair to 0.5 or 1 μM, 5 and 10 μM of each drug. Concentrations of drugs ([D]) that caused a half-maximal inhibition (IC₅₀) and the Hill coefficients (n_h) of concentration-response relationships were estimated by fitting the data to the equation: g_j , % control = $1/[1 + ([D]/EC_{50})^{n_h}]$ where g_j (% control) is fraction of the conductance (g_j) in the absence and presence of the drug. Data are presented as means ± S.E.M.

Experiments on K⁺ and Na⁺ channels were performed with an EPC-10 amplifier (HEKA, Lambrecht/Pfalz, Germany) in the whole-cell configuration of the patch-clamp technique with a holding potential of -80 mV. Pipette resistances averaged 2.0 MΩ. Solutions of triarylmethanes in Ringer were freshly prepared directly before the experiments from 10 mM stock solutions in DMSO. The final DMSO concentration never exceeded 1%. For measurements of KCa2 and KCa3.1 currents we used an internal pipette solution containing (in mM): 145 K⁺ aspartate, 2 MgCl₂, 10 HEPES, 10 K₂EGTA, and 5.96 (250 nM free Ca²⁺) or 8.55 CaCl₂ (1 μM free Ca²⁺), pH 7.2, 290–310 mOsm. Free Ca²⁺ concentrations were calculated with MaxChelator assuming a temperature of 25°C, a pH of 7.2 and an ionic strength of 160 mM. To reduce currents from native chloride channels in COS-7 and HEK-293 cells, Na⁺ aspartate Ringer was used as an external solution (in mM): 160 Na⁺ aspartate, 4.5 KCl, 2 CaCl₂, 1 MgCl₂, 5 HEPES, pH 7.4, 290–310 mOsm. KCa2 and KCa3.1 currents were elicited by 200-ms voltage ramps from -120 to 40 mV applied every 10 s and the fold-increase of slope conductance at -80 mV by drug taken as a measure of channel activation.

KCa1.1 currents were elicited by 200-ms voltage steps from -80 to 60 mV applied every 10 s (1 μM free Ca²⁺), and channel modulation measured as a change in mean current amplitude. Kv1.1, Kv1.3, Kv1.4, Kv1.5, Kv3.1, Kv3.2, and Kv4.2 currents were recorded in normal Ringer solution with a Ca²⁺-free pipette

solution containing (in mM): 145 KF, 10 HEPES, 10 EGTA, 2 MgCl₂, pH 7.2, 300 mOsm. Currents were elicited by 200-ms depolarizing pulses to 40 mV applied every 10 s. HERG (Kv11.1) currents were recorded with a KCl-based pipette solution (4 mM ATP) and with a two-step pulse from -80 mV first to 20 mV for 2 s and then to -50 mV for 2 s. The reduction of both peak and tail current by the drug was determined. Current from co-expressed Kv7.2/7.3 channels was elicited by depolarizing pulses from the holding potential (-80 mV) to +40 mV for 500 ms followed by hyperpolarization to -120 mV for 200 ms. Nav1.2 currents from N1E-115 cells and Nav1.4 currents from stably transfected HEK cells were recorded with 20 ms pulses from -80 to -10 mV every 10 s with a KCl-based pipette solution and normal Ringer as an external solution. Blockade of Na⁺ current was determined by measuring the reduction of peak maximum conductance.

RESULTS

SCREENING OF A "FOCUSED" LIBRARY FOR CX50 INHIBITORS

To identify Cx50 inhibitors we first screened a small library of compounds containing known ion channel pharmacophores including the antihistamine astemizole, several psoralens and related heterocycles, benzothiazoles, triterpenes, and flavanoid glycosides as well as the antifungal agent clotrimazole. From this library we identified four novel low micromolar inhibitors of Cx50: Astemizole, rutin (a flavanoid glycoside), PAA-10 (an alkyl substituted dibenzazocinone), and clotrimazole (see **Figure 1** for structures). All compounds produced significant inhibition of the Cx50 junctional current at a concentration of 10 μM (**Figure 1**). The inhibition of junctional currents caused by clotrimazole, astemizole and PAA-10 was completely reversible upon washout. In contrast, the effects of rutin were only partially reversible. Of these four hits, the triarylmethane clotrimazole seemed the most drug-like and attractive compound to us. Astemizole is known to affect many other ion channels including the cardiac K⁺ channel HERG (Kv11.1; Suessbrich et al., 1996), a liability not generally encountered with triarylmethanes (Toyama et al., 2008). We also discarded rutin as a template since preliminary experiments showed that the rutin aglycon, quercetin, had no effect on Cx50 at 10 μM (data not shown) demonstrating that the sugar moiety is essential for connexin inhibition. The dibenzazocinone PAA-10 would of course also have been a possible lead but we preferred to perform structure activity relationship (SAR) studies around clotrimazole since our laboratory had a library of 80 triarylmethanes that were immediately available for an SAR analysis on Cx50. These compounds had been previously synthesized for an SAR study to determine the structural requirements for inhibition of the intermediate-conductance calcium-activated potassium channel KCa3.1 (a.k.a. IKCa1, SK4). By using the so-called selective optimization of side activities (SOSA) approach, which allows for the selective optimization of the side activity of an old drug (Wermuth, 2004), our group successfully designed a triarylmethane, TRAM-34 (T34), that selectively blocked KCa3.1 channels without affecting cytochrome P450-dependent enzymes, the main target of clotrimazole (Wulff et al., 2000). This previous work had demonstrated that it is possible to achieve selectivity for different targets by appropriately modifying the triarylmethane (TRAM) pharmacophore, which was another reason for

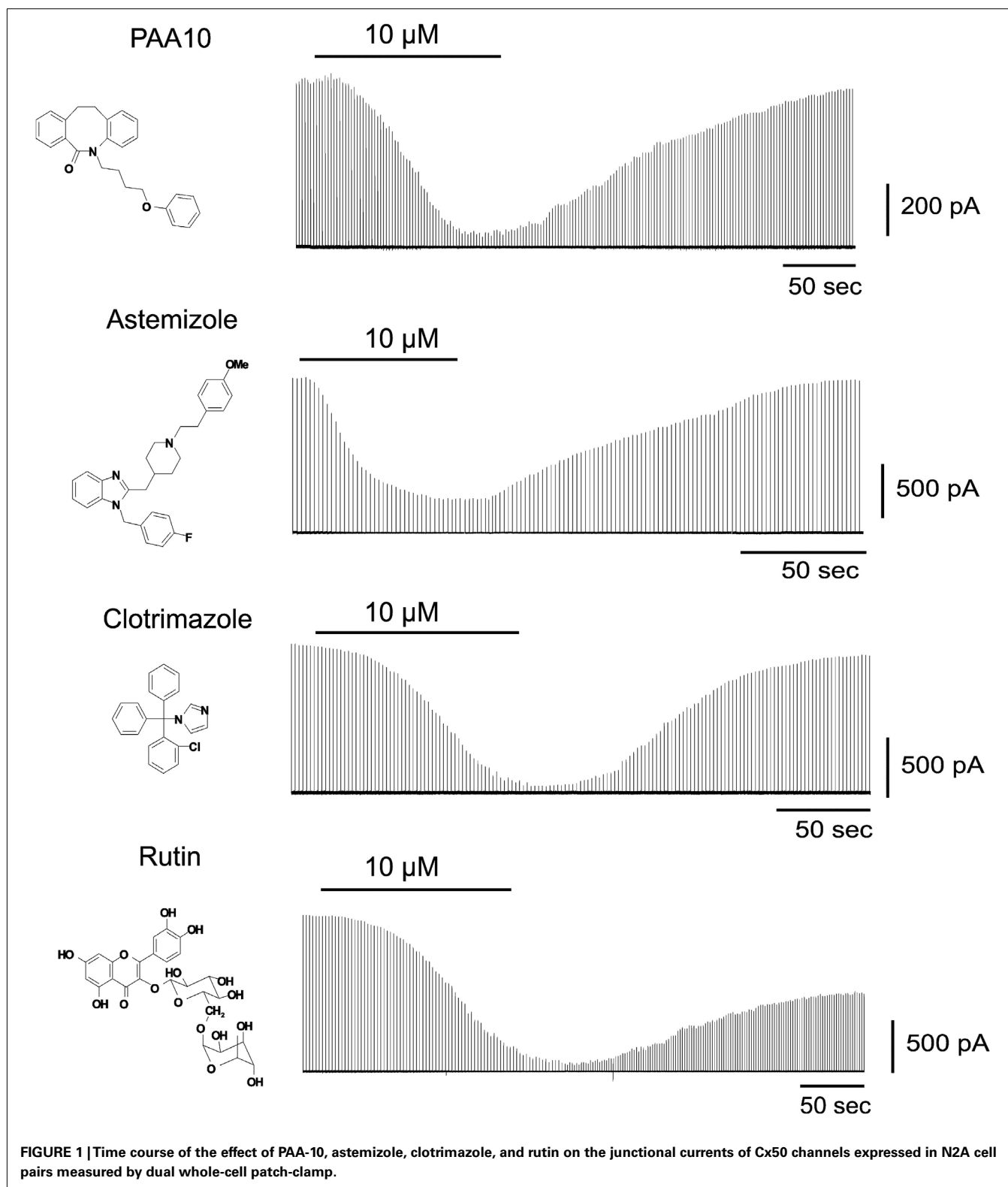
us to choose clotrimazole as a template for our current study on Cx50.

Clotrimazole reversibly inhibited Cx50 expressed in N2A cells with an IC₅₀ of 5 μM and a Hill slope of ~ 2.1 (**Figure 2**). At concentrations of 10 μM clotrimazole had no effect on channels built out of Cx32, Cx36, and Cx46 (**Figure 2**). GJ channel conductance in all cases was measured by using the dual whole-cell patch-clamp technique as described in the Section "Materials and Methods" (Srinivas et al., 2001; Srinivas and Spray, 2003; Cruikshank et al., 2004).

PROBING OF THE TRIARYLMETHANE PHARMACOPHORE FOR CX50 INHIBITION

Using clotrimazole as a template we explored the SAR of the triphenylmethane scaffold according to the synthetic strategy shown in **Figure 3**. In a Grignard reaction mono-substituted benzophenones and bromobenzenes were reacted in anhydrous diethyl ether to yield the corresponding triphenylmethanols. These alcohols were then either ammonolyzed, cyanated with copper cyanide or chlorinated using acetyl chloride. The triphenylmethane chlorides were further reacted in a nucleophilic substitution to give the respective triphenylmethane derivatives (further details on exact conditions and quantities are given in the see Materials and Methods). We first substituted the imidazole ring of clotrimazole with several other heterocycles, differently substituted carbocycles or aliphatic functional groups while keeping the 2-chlorophenyldiphenyl methane basic structure (**Figure 3**). Except for T44 (pyrrol), T69 (2-aminopyridine), T89 (4-methyl-2-phenylimidazole) and the bicyclic T71 (phthalimide) and T103 (2-aminobenzothiazole), most of the heterocyclic derivatives blocked Cx50 in the low micromolar range. Spacer linked carbocycles (T102, T104, T106, T107, T109, T150) in contrast showed no effect on Cx50 at concentrations of 10 μM with the exception of T106, which was found to be a weak blocker with an IC₅₀ 10 μM (**Figure 4**). We next tested the heterocyclic substituted triarylmethanes for selectivity over KCa3.1 (**Figure 4**). As previously reported (Wulff et al., 2000), clotrimazole and T34 (= TRAM-34) are nanomolar KCa3.1 blockers, that exhibit IC₅₀ values of 70 and 20 nM, respectively, and are therefore not useful as Cx50 inhibitors. In contrast, the aminothiazole and aminopyrimidine substituted T66 and T68 were found to be 15- to 200-fold less potent on KCa3.1 and T66 even exhibited a moderate three-fold selectivity for Cx50 over KCa3.1.

Since the alcohol T3, which is the first-step intermediate for the heterocyclic substituted triarylmethanes, was also found to reduce Cx50 currents with an IC₅₀ of 2 μM we further synthesized and tested several triarylmethane alcohols, amines, nitriles, and ureas on Cx50 (**Table A1** in Appendix). While several of the alcohols including the p-chloro substituted T1, the m-chlorosubstituted T2 as well as the non-substituted triphenylmethanol and triphenylamine (T162) exhibited IC₅₀ values for Cx50 in the 1–2 μM range (**Table A1** in Appendix), all these compounds lacked selectivity over KCa3.1 and were further found to inhibit other connexins like Cx43, Cx46 at similar concentrations as Cx50 (data not shown). In addition, the inhibition produced by these compounds was often enhanced by a prior application of the compounds. We therefore did not study these compounds further and instead



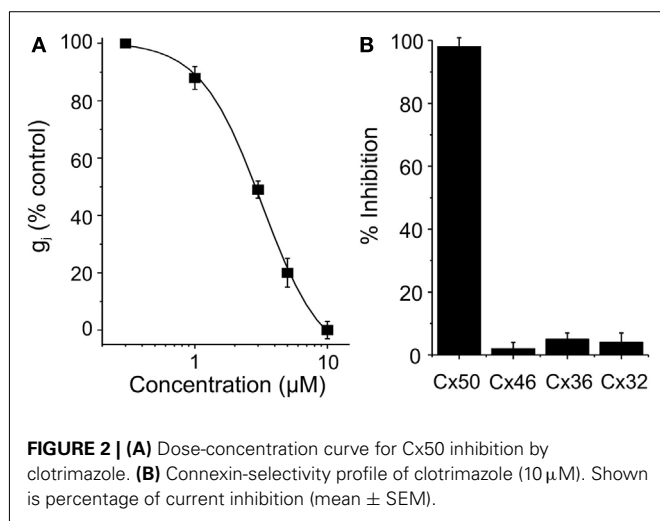
concentrated our synthetic efforts on the heterocyclic substituted triarylmethanes and explored the substitution position of the chlorine atom on one of the phenyl rings by moving it from the ortho to the meta- or para-position or completely removing it (Figure 5).

All four imidazole ring containing compounds (T97, clotrimazole, T143, T144) but only the o-chloro and m-chloro substituted pyrazole derivatives (T34 and T142) inhibited Cx50 channels with IC_{50} s of 5–8 μ M. In the 2-aminothiazole and 2-aminopyrimidine

series only the *o*-chloro substituted T66 and T68 were active, while the other regio-isomers or the unsubstituted analogs showed no effect at 10 μ M. Because the imidazole and pyrazole-substituted triarylmethanes were poorly selective for Cx50 over KCa3.1, we studied the effect of modifications of the *o*-chloro substituent in the 2-aminothiazole and 2-aminopyrimidine series. Specifically, we replaced the *o*-chloro substituent with other halogens (F, Br, I), the more lipophilic CF₃ or OCF₃ groups or electron-donating methyl or methoxy groups. All 14 compounds exhibited IC₅₀ values in the low micromolar range (Figure 6) with the methoxy-substituted T122 (IC₅₀ 1.2 μ M) and the iodo-substituted T136 (IC₅₀ 2.4 μ M) being the most potent (Figure 6).

T122 AND T136 ARE SELECTIVE FOR CX50

The effects of T122 and T136 on Cx50 junctional channels were further characterized using a five-point dose response curve (Figure 7A). Non-linear least-squares fit of the individual data



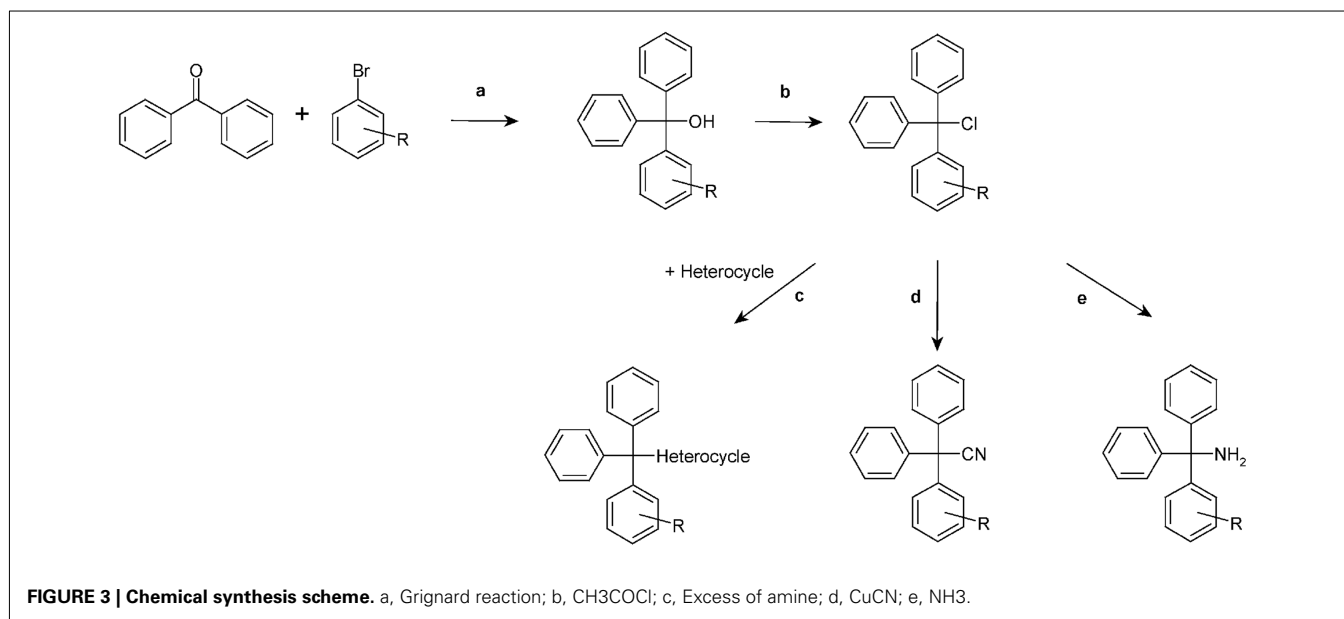
points to the Hill equation (see Materials and Methods) yielded IC₅₀ values of 1.2 and 2.4 μ M for the inhibition of Cx50 GJ channels by T122 and T136, respectively. In both cases, the Hill coefficients were \approx 2 (1.6 for T122, 1.7 for T136), indicating that binding of two TRAM molecules was required to inhibit Cx50 GJ channels. Both compounds exhibited high selectivity for Cx50 channels over other connexin subtypes. The effects of T122 and T136 on GJ channels formed by several other connexins, including Cx26, Cx32, Cx40, Cx43, and Cx46 are illustrated in Figure 7B. At a concentration of 10 μ M, sufficient to cause near-maximal decreases in Cx50 junctional current, T122 and T136 did not significantly inhibit Cx26, Cx32, Cx46, or Cx43 GJ channel currents. The reduction of junction conductance was less than 20% in each of these cases. These results demonstrate that inhibition of Cx50 GJ channels by T122 and T136 is highly connexin-selective.

SELECTIVITY OVER Kv, K_{Ca}, AND Nav CHANNELS

In order to more broadly evaluate the selectivity of T122 and T136 we further determined their effect on a panel of 12 potassium and sodium channels from various gene families (Table 1). While both compounds exerted practically no effect on the neuronal Nav1.2 and the skeletal muscle Nav1.4 channel or Kv channels from the Kv4, Kv7, Kv11, or KCa2 (SK) family, they exhibited only moderate selectivity over Kv1, Kv2, Kv3-family channels, Kv11.1 (hERG), and the calcium-activated K⁺ channels KCa1.1 and KCa3.1. T122 in particular reduced Kv1.1 currents by 65% at 10 μ M, while T136 was found to have an IC₅₀ of 1.3 μ M for KCa3.1.

T122 AND T136 INHIBIT COUPLING IN THE LENS

Cx50 is strongly expressed in the lens in both the epithelium and in fibers. In the epithelium, the functional contribution of Cx50 to epithelial cell coupling is highest during the first postnatal week (\sim 70–75% of total coupling on average) with the remainder being contributed by Cx43. Therefore, we determined whether T122 and T136 (10 μ M) also inhibited coupling



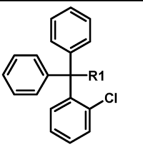
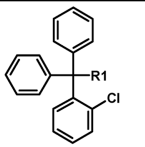
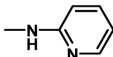
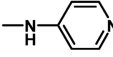
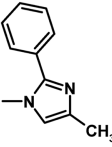
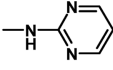
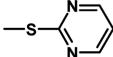
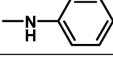
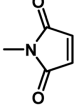
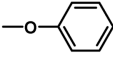
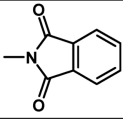
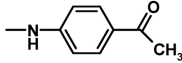
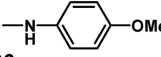
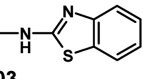
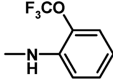
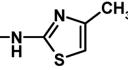
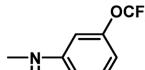
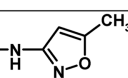
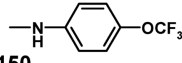
 R1 =	IC ₅₀ Cx50 [μM]	IC ₅₀ KCa3.1 [μM]	 R1 =	IC ₅₀ Cx50 [μM]	IC ₅₀ KCa3.1 [μM]
 Clotrimazole	5	0.07	 T69	No effect	28
 T85	4.2	> 20	 T67	5	30
 T89	No effect	> 20	 T68	8	14
 T34	8.3	0.02	 T112	8	Not tested
 T44	No effect	7	 T109	No effect	Not tested
 T91	7.3	Not tested	 T107	No effect	Not tested
 T71	No effect	No effect	 T150	No effect	Not tested
 T66	3	15	 T106	10	Not tested
 T103	No effect	Not tested	 T104	No effect	Not tested
 T79	5.5	8	 T102	No effect	Not tested
 T80	11	1	 T150	No effect	Not tested

FIGURE 4 | Table showing the structures and IC₅₀ values for Cx50 and KCa3.1 inhibition of heterocyclic substituted triarylmethanes.

Concentrations of triarylmethanes that caused a half-maximal inhibition (IC₅₀) values were obtained by fitting the data to the Hill equation, as described in

the methods. Means of current inhibition and SD were determined by application of two or three concentrations of each triarylmethane to multiple cells (*n* ranging from 3 to 8 per concentration). The SD values are not shown for clarity; SD values typically ranged between 5 and 15%.

provided by Cx50 in epithelial cells (Figure 8). The effect of T122 and T136 on junctional currents between epithelial cells isolated from mouse lenses on postnatal day 6 is shown in Figure 8A. Both compounds strongly reduced junctional currents, an effect that was reversible on washout of the drug. The reduction of junctional currents caused by T122 and T136 ranged from 65 to 87% of the initial conductance (means ± SEM are 67 ± 9%, *n* = 7 for T122; and 64 ± 8%, *n* = 6 for T136).

These values were similar to the reduction produced by quinine, which also selectively inhibits Cx50, but not Cx43 GJ channels (Figure 8B).

DISCUSSION

A major reason for the poorly developed pharmacology of GJ channel modulators is the intercellular location of these channels, which makes it extremely difficult to design high-throughput

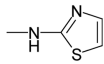
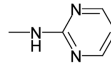
		R1 =			
					
Position of -Cl	/	T97 5.1 μ M	T11 No effect	T57 No effect	T141 No effect
	ortho	Clotrimazole 5 μ M	T34 8.3 μ M	T66 3 μ M	T68 8 μ M
	meta	T143 4.3 μ M	T142 7.1 μ M	T129 No effect	T130 No effect
	para	T144 6.1 μ M	T13 No effect	T64 No effect	T145 No effect

FIGURE 5 | Table showing the structures and IC_{50} values for Cx50 inhibition for imidazole, pyrazole, aminothiazole, and aminopyrimidine substituted triarylmethanes bearing a chlorine substituent in various positions on one of the phenyl rings. Means of current inhibition and SD

were determined by application of two or three concentrations of each triarylmethane to multiple cells (n ranging from 3 to 8 per concentration). The SD values are not shown for clarity; SD values typically ranged between 5 and 15%.

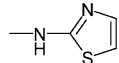
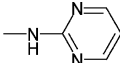
		R1 =	
			
R2 =			
F	T78 8.3 μ M	T128 9 μ M	
Cl	T66 3 μ M	T68 8 μ M	
Br	T131 3.2	T132 8 μ M	
I	T136 2.4	T137 2.6	
CF ₃	T72 5 μ M	T73 3 μ M	
OCF ₃	T126 7.4 μ M	T127 5.1 μ M	
CH ₃	T124 7.2 μ M	T125 No effect	
OCH ₃	T122 1.2 μ M	T123 3 μ M	

FIGURE 6 | Table showing the structures and IC_{50} values for Cx50 inhibition for aminothiazole and aminopyrimidine substituted triarylmethanes with various functional groups in ortho-position on one of the phenyl rings. Means of current inhibition and SD were determined by application of two or three concentrations of each triarylmethane to multiple cells (n ranging from 3 to 8 per concentration). The SD values are not shown for clarity; SD values typically ranged between 5 and 15%.

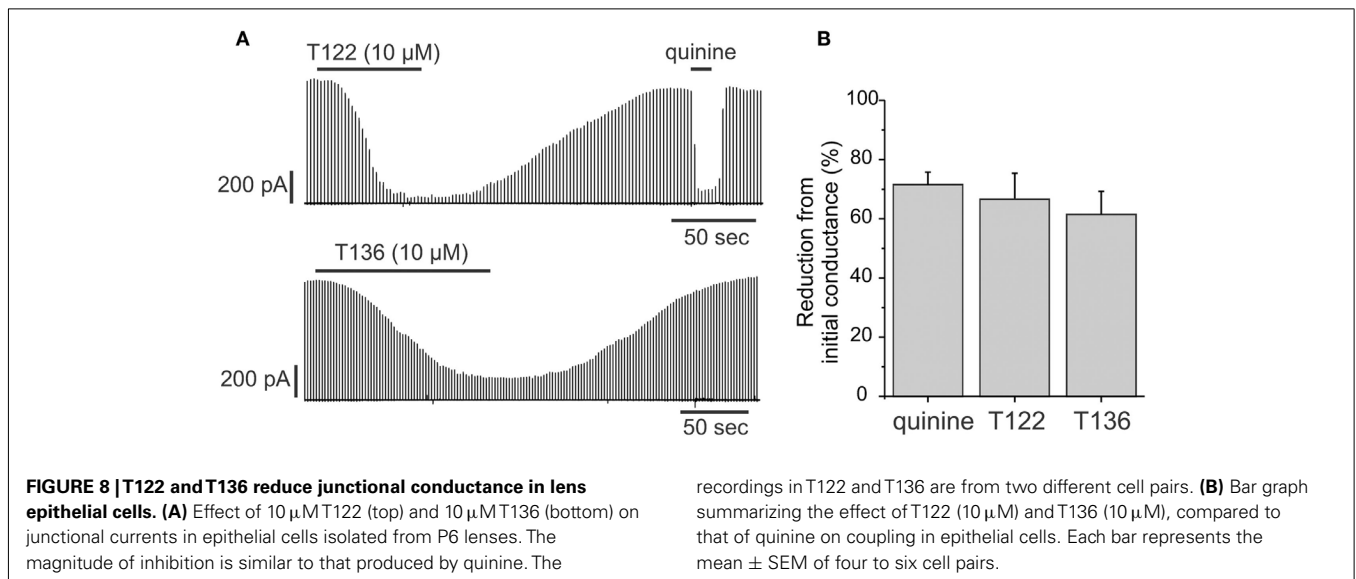
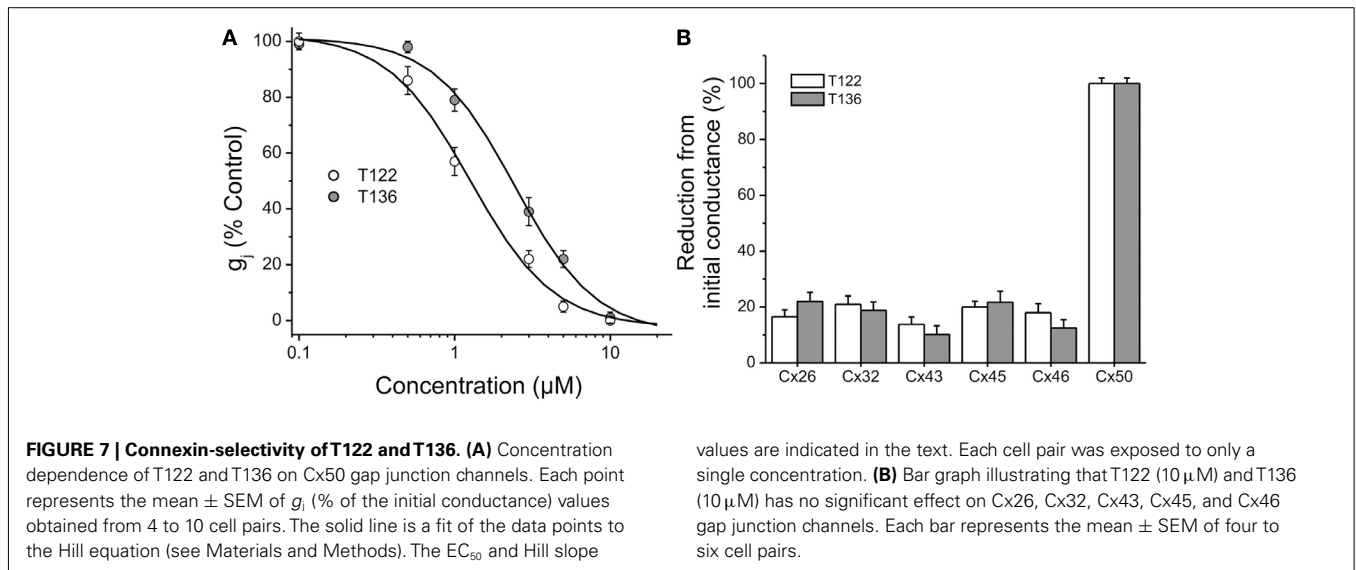
screening assays. In our search for Cx50 inhibitors we therefore decided to screen a small library containing known ion channel modulators using conventional dual whole-cell voltage-clamp. Our library was enriched in so-called “privileged” structures which are small molecule pharmacophores that are able to bind to multiple targets and which are therefore highly likely to exert biological effects (Evans et al., 1988; Horton et al., 2003). By appropriately decorating such “privileged” scaffolds their potency and selectivity can often be directed toward a single target with relatively

Table 1 | Selectivity over other ion channels.

Channel	T122 (10 μ M)	T136 (10 μ M)
Kv1.1	65 \pm 10% block (n = 5)	28 \pm 9% block (n = 5)
Kv1.3	52 \pm 2% block (n = 3)	18 \pm 4% block (n = 3)
Kv2.1	28 \pm 4% block (n = 3)	28 \pm 4% block (n = 3)
Kv3.1	32 \pm 12% block (n = 5)	37 \pm 16% block (n = 4)
Kv4.2	16 \pm 4% block (n = 3)	15 \pm 3% block (n = 3)
Kv7.2/7.3	No effect (n = 3)	No effect (n = 2)
Kv11.1 (hERG)	42 \pm 3% block (n = 3)	27 \pm 4% block (n = 3)
KCa2.3	No effect (n = 3)	No effect (n = 3)
KCa3.1	IC_{50} = 10.2 \pm 0.7 μ M	IC_{50} = 1.3 \pm 0.2 μ M
KCa1.1 (BK)	43 \pm 4% (n = 3)	26 \pm 2% (n = 3)
Nav1.2	11 \pm 1% block (n = 3)	9 \pm 0.5% block (n = 3)
Nav1.4	No effect (n = 3)	No effect (n = 3)

Percentage of current inhibition (mean \pm SD) by 10 μ M T122 and T136 for a panel of cloned Kv, K_{Ca}, or Nav channels. (For recording conditions and pulse protocols see Materials and Methods).

high affinity. If the template for such an SAR study is an “old” drug, the approach is also called SOSA approach (selective optimization of the side activity of an old drug) as suggested by Wermuth (2004). Using this approach we found four structurally very different compounds able to inhibit Cx50 channels in the low micromolar range including the triarylmethane (TRAM) clotrimazole (IC_{50} 5 μ M; **Figure 1**). Using clotrimazole as a template, we have tested a series of previously known or newly synthesized differently substituted TRAMs for their effects on Cx50 channels and identified several compounds inhibiting Cx50 in the low micromolar range including T122, which exhibits an IC_{50} of 1.2 μ M for Cx50 and excellent selectivity over other connexins. Analyzing at the structural requirements for selective Cx50 inhibition we find that the TRAM pharmacophore should contain a heteroaromatic ring system in R1 position. Smaller, less bulky substitutions with functional groups such as OH, NH, or H also result in potent Cx50 blockers (**Table A1** in Appendix), however, these types of compounds lack selectivity over other connexins and are therefore not useful as pharmacological tools. In addition to a



heteroaromatic substituent in R1 position, the second requirement is that one of the phenyl rings of the triphenylmethane should be substituted preferably in ortho-position (**Figure 5**), whereby it seems to be of little consequence whether the substituent is electron withdrawing (CF₃ in T72) or donating (OCH₃ in T122), as long as it is lipophilic. Lastly, the heteroaromatic ring system, which can be directly attached or linked by a one-atom spacer (nitrogen or sulfur), should contain at least one hydrogen-bond accepting heteroatom, which might be directly interacting with a hydrogen-bond donor in the connexin protein (e.g., see clotrimazole with its imidazole ring versus the inactive T44 and T109). It also seems that steric bulk is a limiting factor for potency, because the bulkier bicyclic derivatives T103 and T71 are ineffective while the smaller T66 and T91 inhibit Cx50.

Since our compounds were derived from clotrimazole, which inhibits KCa3.1 channels with an IC₅₀ of 70 nM, we also tested the more active compounds for selectivity over KCa3.1. For nanomolar KCa3.1 inhibition Wulff et al. (2000) previously proposed a propeller-shaped pharmacophore consisting of the triphenyl moiety with an o-halogen on one of the phenyl rings and an unsubstituted, polar π -electron-rich heterocycle of limited size such as pyrazole, tetrazole, or an even smaller nitrile group in R1 position. A similar KCa3.1-inhibiting TRAM pharmacophore was described by McNaughton-Smith et al. (2008) as exemplified by ICA-17043 (Senicapoc®), which contains a carboxamide moiety in R1 position and entered clinical trials for sickle cell anemia. Considering this knowledge about the TRAM pharmacophore for KCa3.1 inhibition in our current Cx50-focused SAR study, we could achieve a drop in potency on KCa3.1 of more

than 1000-fold by inserting a one-atom linker between the triphenyl moiety and the heterocycle in R1 position. This insertion, which results in a “kink” in the perfect propeller shape of clotrimazole or TRAM-34 shifted selectivity toward Cx50 [clotrimazole (IC₅₀ of 70 nM for KCa3.1 and 5 μM Cx50) versus T122 (IC₅₀ of 10 μM for KCa3.1 and 1.2 μM for Cx50)]. At concentrations of 10 μM the two most potent compounds, T122 and T136, showed excellent selectivity over other tested connexin channels including channels built out of Cx43 and Cx46, which are also expressed in the lens (inhibition < 18%). In addition, T122 and T136 showed very good selectivity over sodium channels (<11%) and moderate selectivity over most of the tested potassium channels (18–43%), except for T122, which blocked Kv1.1 by 65%. Both compounds also inhibited Cx50 mediated coupling in primary lens epithelial cells. Thus, compared to the existing pharmacological agents such as quinine and 2-APB, which exhibit poor selectivity for Cx50 channels, T122 and T136 are likely better agents for studying the role of Cx50 in lens development and the maintenance of lens transparency.

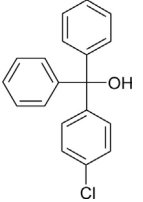
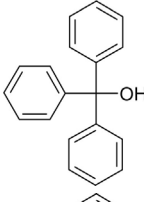
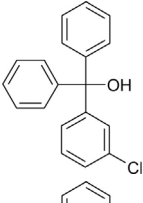
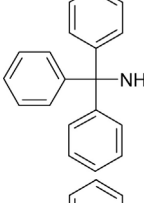
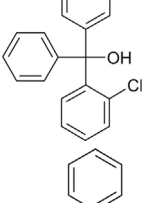
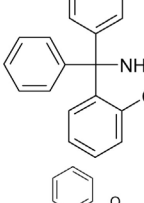
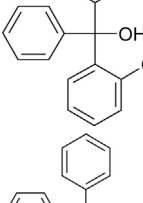
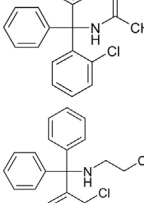
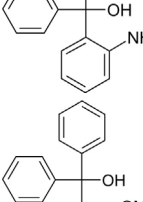
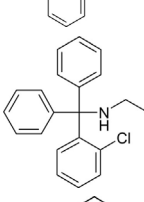
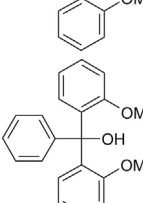
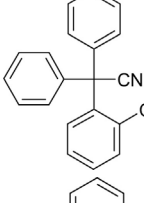
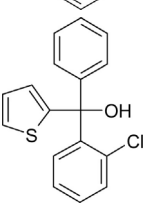
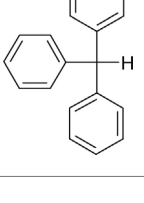
REFERENCES

- Baeyer, A. (1907). The investigation of derivatives of triphenylcarbinol. First paper. *Justus Liebigs Ann. Chem.* 354, 152–204.
- Bartroli, J., Alguero, M., Boncompte, E., and Forn, J. (1992). Synthesis and antifungal activity of a series of difluorotriylimidazoles. *Arzneimittelforschung* 42, 832–835.
- Berthoud, V. M., and Beyer, E. C. (2009). Oxidative stress, lens gap junctions, and cataracts. *Antioxid. Redox Signal.* 11, 339–353.
- Bodendiek, S. B., and Raman, G. (2010). Connexin modulators and their potential targets under the magnifying glass. *Curr. Med. Chem.* 17, 4191–4230.
- Cruikshank, S. J., Hopperstad, M., Younger, M., Connors, B. W., Spray, D. C., and Srinivas, M. (2004). Potent block of Cx36 and Cx50 gap junction channels by mefloquine. *Proc. Natl. Acad. Sci. U.S.A.* 101, 12364–12369.
- Dahlbom, R., and Ekstrand, T. (1944). Trityl derivatives of sulfanilamides. *Sven Kem. Tidskr.* 56, 304–314.
- Evans, B. E., Rittle, K. E., Bock, M. G., DiPardo, R. M., Freidinger, R. M., Whitter, W. L., Lundell, G. F., Veber, D. F., Anderson, P. S., and Chang, R. S. (1988). Methods for drug discovery: development of potent, selective, orally effective cholecystokinin antagonists. *J. Med. Chem.* 31, 2235–2246.
- Gomberg, M., and Van Slyke, D. D. (1911). Triphenylmethyl. *XX. J. Am. Chem. Soc.* 33, 531–549.
- Grissmer, S., Nguyen, A. N., Aiyar, J., Hanson, D. C., Mather, R. J., Gutman, G. A., Karmilowicz, M. J., Auperin, D. D., and Chandy, K. G. (1994). Pharmacological characterization of five cloned voltage-gated K⁺ channels, types Kv1.1, 1.2, 1.3, 1.5, and 3.1, stably expressed in mammalian cell lines. *Mol. Pharmacol.* 45, 1227–1234.
- Horton, D. A., Bourne, G. T., and Smythe, M. L. (2003). The combinatorial synthesis of bicyclic privileged structures or privileged substructures. *Chem. Rev.* 103, 893–930.
- Kandouz, M., and Batist, G. (2010). Gap junctions and connexins as therapeutic targets in cancer. *Expert Opin. Ther. Targets* 14, 681–692.
- Lang, N. N., Myles, R. C., Burton, F. L., Hall, D. P., Chin, Y. Z., Boon, N. A., and Newby, D. E. (2008). The vascular effects of rosiglitazone in vivo in man. *Biochem. Pharmacol.* 76, 1194–1200.
- Locovei, S., Scemes, E., Qiu, F., Spray, D. C., and Dahl, G. (2007). Pannexin1 is part of the pore forming unit of the P2X(7) receptor death complex. *FEBS Lett.* 581, 483–488.
- Mathias, R. T., Rae, J. L., and Baldo, G. J. (1997). Physiological properties of the normal lens. *Physiol. Rev.* 77, 21–50.
- Mathias, R. T., White, T. W., and Gong, X. (2010). Lens gap junctions in growth, differentiation, and homeostasis. *Physiol. Rev.* 90, 179–206.
- McNaughton-Smith, G. A., Burns, J. F., Stocker, J. W., Rigdon, G. C., Creech, C., Arrington, S., Shelton, T., and de Franceschi, L. (2008). Novel inhibitors of the Gardos channel for the treatment of sickle cell disease. *J. Med. Chem.* 51, 976–982.
- Misra, B. K., Rao, Y. R., and Mahapatra, S. N. (1983). Friedel-Crafts acylation of some aromatic compounds with 2-isocyanatobenzoyl chloride. *Indian J. Chem. Sect. B* 22B, 1132–1138.
- Monder, C., Stewart, P. M., Lakshmi, V., Valentino, R., Burt, D., and Edwards, C. R. (1989). Licorice inhibits corticosteroid 11 beta-dehydrogenase of rat kidney and liver: in vivo and in vitro studies. *Endocrinology* 125, 1046–1053.
- Nemani, V. M., and Binder, D. K. (2005). Emerging role of gap junctions in epilepsy. *Histol. Histopathol.* 20, 253–259.
- Rong, P., Wang, X., Niesman, I., Wu, Y., Benedetti, L. E., Dunia, I., Levy, E., and Gong, X. (2002). Disruption of Gja8 (alpha 8 connexin) in mice leads to microphthalmia associated with retardation of lens growth and lens fiber maturation. *Development* 129, 167–174.
- Salameh, A., and Dhein, S. (2005). Pharmacology of gap junctions. New pharmacological targets for treatment of arrhythmia, seizure and cancer? *Biochim. Biophys. Acta* 1719, 36–58.
- Sankaranarayanan, A., Raman, G., Busch, C., Schultz, T., Zimin, P. I., Hoyer, J., Kohler, R., and Wulff, H. (2009). Naphtho[1,2-d]thiazol-2-ylamine (SKA-31), a new activator of KCa2 and KCa3.1 potassium channels, potentiates the endothelium-derived hyperpolarizing factor response and lowers blood pressure. *Mol. Pharmacol.* 75, 281–295.
- Srinivas, M., Hopperstad, M. G., and Spray, D. C. (2001). Quinine blocks specific gap junction channel subtypes. *Proc. Natl. Acad. Sci. U.S.A.* 98, 10942–10947.
- Srinivas, M., and Spray, D. C. (2003). Closure of gap junction channels by arylaminobenzoates. *Mol. Pharmacol.* 63, 1389–1397.
- Suadicani, S. O., Brosnan, C. F., and Scemes, E. (2006). P2X7 receptors mediate ATP release and amplification of astrocytic intercellular Ca²⁺ signaling. *J. Neurosci.* 26, 1378–1385.
- Suessbrich, H., Waldegger, S., Lang, F., and Busch, A. E. (1996). Blockade of HERG channels expressed in *Xenopus* oocytes by the histamine receptor antagonists terfenadine and astemizole. *FEBS Lett.* 385, 77–80.
- Toyama, K., Wulff, H., Chandy, K. G., Azam, P., Raman, G., Saito, T., Fujiwara, Y., Mattson, D. L., Das, S., Melvin, J. E., Pratt, P. F., Hatoum, O. A., Gutterman, D. D., Harder, D. R., and Miura, H. (2008). The intermediate-conductance calcium-activated potassium channel KCa3.1 contributes to atherogenesis in mice and humans. *J. Clin. Invest.* 118, 3025–3037.
- Vessey, J. P., Lalonde, M. R., Mizan, H. A., Welch, N. C., Kelly, M. E., and Barnes, S. (2004). Carbenoxolone inhibition of voltage-gated Ca channels and synaptic transmission in the retina. *J. Neurophysiol.* 92, 1252–1256.
- Wermuth, C. G. (2004). Selective optimization of side activities: another way for drug discovery. *J. Med. Chem.* 47, 1303–1314.

- White, T. W., Gao, Y., Li, L., Sellitto, C., and Srinivas, M. (2007). Optimal lens epithelial cell proliferation is dependent on the connexin isoform providing gap junctional coupling. *Invest. Ophthalmol. Vis. Sci.* 48, 5630–5637.
- White, T. W., Goodenough, D. A., and Paul, D. L. (1998). Targeted ablation of connexin50 in mice results in microphthalmia and zonular pulverulent cataracts. *J. Cell. Biol.* 143, 815–825.
- Wulff, H., Gutman, G. A., Cahalan, M. D., and Chandy, K. G. (2001). Delineation of the clotrimazole/TRAM-34 binding site on the intermediate conductance calcium-activated potassium channel IKCa1. *J. Biol. Chem.* 276, 32040–32045.
- Wulff, H., Miller, M. J., Haensel, W., Grissmer, S., Cahalan, M. D., and Chandy, K. G. (2000). Design of a potent and selective inhibitor of the intermediate-conductance Ca²⁺-activated K⁺ channel, IKCa1: a potential immunosuppressant. *Proc. Natl. Acad. Sci. U.S.A.* 97, 8151–8156.
- Zunzain, P. A., Shah, M. M., Miscony, Z., Javadzadeh-Tabatabaie, M., Haylett, D. G., and Ganellin, C. R. (2002). Tritylamino aromatic heterocycles and related carbinols as blockers of Ca²⁺-activated potassium ion channels underlying neuronal hyperpolarization. *Arch. Pharm.* 335, 159–166.
- Conflict of Interest Statement:** The authors declare that the research was conducted in the absence of any commercial or financial relationships that could be construed as a potential conflict of interest.
- Received: 20 March 2012; accepted: 18 May 2012; published online: 06 June 2012.
- Citation: Bodendiek SB, Rubinos C, Trelles MP, Coleman N, Jenkins DP, Wulff H and Srinivas M (2012) Triarylmethanes, a new class of Cx50 inhibitors. *Front. Pharmacol.* 3:106. doi: 10.3389/fphar.2012.00106
- This article was submitted to *Frontiers in Pharmacology of Ion Channels and Channelopathies*, a specialty of *Frontiers in Pharmacology*.
- Copyright © 2012 Bodendiek, Rubinos, Trelles, Coleman, Jenkins, Wulff and Srinivas. This is an open-access article distributed under the terms of the Creative Commons Attribution Non Commercial License, which permits non-commercial use, distribution, and reproduction in other forums, provided the original authors and source are credited.

APPENDIX

Table A1 | IC₅₀ values for Cx50 inhibition for triarylmethane alcohols, amines, nitriles and ureas.

	Compound	IC ₅₀ Cx50 (μM)	IC ₅₀ KCa3.1 (μM)		Compound	IC ₅₀ Cx50 (μM)	IC ₅₀ KCa3.1 (μM)
T1		2.8	0.53	Triphenylmethanol		1	0.5
T2		3.6	0.55	T162		1.5	5.3
T3		2	0.52	T41		4	1
T54		3	0.7	T75		No effect	1.2
T154-OH		No effect	N/A	T95		6	5
T117		No effect	N/A	T94		73	Not tested
T165		No effect	N/A	T39		4	0.06
T43		2	0.75	Triphenylmethane		0.9	3.7

(Continued)

(Continued)

Table A1 | Continued

Compound	IC ₅₀ Cx50 (μM)	IC ₅₀ KCa3.1 (μM)
T51	No effect	25
T24	No effect	8
T74	No effect	4
T52	10	>50
T53	10	>50
T50	10	>50
T160	4	8.6
T9	4	1.5
T35	10	9